

CONTROL OF SHIP'S ROLL BY ACTIVE FIN STABILIZERS

A DISSERTATION

*Submitted in partial fulfillment of the
requirement for the award of the degree
of*

**MASTER OF TECHNOLOGY
in
ELECTRICAL ENGINEERING
(With Specialization in System and Control)**

**By
THVVRN SUNIL**



**DEPARTMENT OF ELECTRICAL ENGINEERING
INDIAN INSTITUTE OF TECHNOLOGY ROORKEE
ROORKEE, INDIA - 247667**

MAY 2016

CANDIDATE'S DECLARATION

I hereby certify that this report which is being presented in the dissertation titled “**Control of Ship's Roll by Active Fin Stabilizers**” in partial fulfillment of the requirement of award of Degree of **Master of Technology in Electrical Engineering** with specialization in **System And Control**, submitted to the Department of Electrical Engineering, Indian Institute of Technology, Roorkee, India is an authentic record of the work carried out during a period from Jun 2015 to May 2016 under the supervision of **Dr. Rajendra Prasad**, Department of Electrical Engineering, Indian Institute of Technology, Roorkee. The matter presented in this mid-dissertation report has not been submitted by me for the award of any other degree of this institute or any other institute.

Date : May 2016

Place : Roorkee

(THVVRN Sunil)

Enrl No:14530020

CERTIFICATE

This is to certify that the above statement made by the candidate is correct to best of my knowledge.

(Dr. Rajendra Prasad)

Professor

Department of Electrical Engineering

Indian Institute of Technology Roorkee

Roorkee, India -247667

ACKNOWLEDGEMENT

I wish to express my deep regards and sincere gratitude to my respected guide dr. Rajendra Prasad, Professor, Department of Electrical Engineering, Indian Institute of Technology, Roorkee for being helpful and a great source of inspiration. His keen interest and constant encouragement gave me the confidence to complete my work. I wish to extend my sincere thanks for his excellent guidance and suggestions for the successful completion of my work.

THVVRN Sunil

ABSTRACT

Stabilization of ship roll motion induced by wave disturbances is one of the important controls required in the modern day marine industry. Excessive roll motion makes the ship's crew uncomfortable and also causes damage to the cargoes and equipment on board. Active-fin stabilisers are the most widely used equipments out of the many other available stabilizers like anti-roll tanks, gyroscope and bilge keel in today's marine world to reduce the roll motion. It rotates about its stock to give a desired hydrodynamic list to stabilize the ship's roll.

Various control strategies have been used for the roll motion control of ships. However, most of the research includes stabilization of a ship with fixed mathematical model. The major **changes in the ship's parameters** like weight and meta-centric height **due to practical reasons** are generally not considered for controller design. This dissertation exploits this fact to study, analyze and design a controller for the ship with varied parameters including weight of the ship.

In this dissertation, three different conditions of a ship model are selected and PID controllers were separately designed for all the 3 conditions. These PID controllers are amalgamated to design a neural network controller. Thereafter, neural network controller is improved upon in various steps to arrive at an optimal controller to control the ship's roll in all the three possible conditions of the ship. The neural network controller could successfully **control even the sinking ship**.

There is a **saturation limit for the stabilizer fin angle** which is generally not considered by many researchers in their work or simulations. In this dissertation even the non-linearity in the form of fin angle's saturation is considered during the design of PID/NN/FL controllers. Performance of a controller may decrease by considering fin's angle saturation. However this is what is practical and **designing controllers without considering saturation limit is meaningless** and is of no practical use.

After the design of the NN controller, the creation of a fuzzy logic controller was envisaged. In the pursuit to make the best possible FLC even with non-availability of the system information for the rule creation, data from the previously designed 3 PID controller was used to frame the rules. Various FLCs with **varied shapes, sizes and calculated parameters of the membership functions** of the fuzzy sets were created, tested and analyzed. Some of the FLCs were even designed with **125 rules along with a separate weightage for each rule**. **Particle swarm optimization** was later used to fine tune the gains added to the Fuzzy logic controller for better control of ship's roll. The finalised FLC also could save the sinking ship and give good performance. FLC also could **reduce roll frequency** to a great extent which is very important for some ships with specific roles.

TABLE OF CONTENTS

Candidate's Declaration.....	ii
Acknowledgement.....	iii
Abstract	iv
Table of contents.....	v
List of Figures.....	vii
List of Tables.....	xi
List of Abbreviations.....	xiii
1. INTRODUCTION.....	1
1.1 Background..	1
1.2 Ship Roll Stabilization Techniques.....	2
1.3 Types of stabilisers.....	2
2. ACTIVE FIN STABILISERS.....	9
2.1 Principle of Operation.....	9
2.2 Direction of Fin Movement.....	10
3. SYSTEM MODELING.....	11
3.1 Various Moments Acting Towards Ship Roll.....	11
3.2 Mathematical model of ship dynamics.....	12
3.3 Wave disturbance model.....	14
3.4 Control System Model.....	15
4. PID CONTROLLER AND RELATED PROBLEMS.....	17
4.1 PID Controller.....	17
4.2 Initial Analysis.....	18
4.3 Parameter Variations / Perturbations in the system:.....	18
4.4 Three types of ship models.....	21
4.5 Stability curve.....	23
5. NEURAL NETWORK.....	25
5.1 Introduction.....	25
5.2 Training of NN Controller.....	25
5.3 Performance of NN Controller.....	26
5.4 Reduction of Statistics of Roll (RSR).....	30

5.5	Neural Network Controller with 2-Inputs.....	30
5.6	Neural Network Controller with 3-Inputs.....	32
5.7	Number of Hidden Neurons.....	35
6.	SATURATION LIMITS OF STABILIZERS FINS.....	40
6.1	Introduction.....	40
6.2	Common Mistake by Researchers.....	40
6.3	Saturation Limits.....	41
7	FUZZY LOGIC CONTROLLER.....	45
7.1	Introduction.....	45
7.2	Shape selection for Membership Functions.....	45
7.3	Fuzzy Logic Controller with 2-Inputs.....	47
7.4	FLC with Different Sized Gaussian Membership Functions.....	53
7.5	FLC With Zero-Centered and Different Sized Gaussian MFs.....	59
7.6	FLC with Different Sized Triangular MFs.....	60
7.7	FLC with Zero-Centered and Different Sized Triangular MFs.....	63
8	PARTICLE SWARM OPTIMIZATION (PSO).....	65
8.1	Introduction.....	65
8.2	PSO for tuning FLC gains.....	65
9	RESULTS AND ANALYSIS.....	68
10	CONCLUSION AND FUTURE WORK.....	71
11.	BIBILIOGRAPHY	73

LIST OF FIGURES

Fig 1.1	Devastating effects of ship's roll.....	1
Fig 1.2	Gyro stabiliser installed on USS Aramis.....	3
Fig 1.3	Bilge Keel for Ship Stabilisation.....	4
Fig 1.4 .	Cut section of Anti-Roll tank (www.hoppe-marine.com).....	4
Fig. 1.5.	Typical fin stabiliser arrangement.....	6
Fig 1.6	Rudders of a ship.....	7
Fig 1.7	Types of Stabilizers.....	8
Fig 2.1	Hydrodynamic Forces acting on Stabilizer Fins.....	9
Fig 2.2	Photo showing relatively small size of stabilizers below waterline.....	9
Fig 2.3	Front and side view of Stabilizer.....	10
Fig 2.4.	Direction of fins motion for both side rolls.....	10
Fig 3.1	Restoring moment is dependent on center of gravity and buoyancy.....	11
Fig 3.2	Righting moment created by stabilizers.....	12
Fig 3.3	Wave disturbance considered for ship's roll motion.....	15
Fig 3.4	Block diagram of the ship's roll control system.....	16
Fig 4.1	Ship's response with the tuned PID controller.....	18
Fig. 4.2	Large portion of ship's weight is its fuel (coloured brown).....	18
Fig 4.3	Ship version of Brahmos missile weighing 3000 kgs.....	19
Fig 4.4	Fishing trawlers with heavy fishing nets.....	19
Fig 4.5	Photo depicting the large size of fishing nets.....	19
Fig 4.6	Cargo ship with and without its large cargo.....	20
Fig 4.7	Change in center of gravity due to free surface effect.....	20
Fig 4.8	Meta-centric height (GMt) of a ship.....	20
Fig 4.9	Corroded ship's hull.....	21

Fig 4.10	Marine growth on ship's bottom surface.....	21
Fig 4.11	Roll angle of ship "A" using PID controller.....	22
Fig 4.12	Roll angle of ship "B" using PID controller.....	22
Fig 4.13	Roll angle of ship "C" using PID controller.....	23
Fig 4.14	A typical stability curve showing righting lever vs roll angle.....	23
Fig 5.1	A simple neural network.....	25
Fig 5.2	Training of NN controller with one input and one target.....	26
Fig 5.3	Ship's roll control using NN controller.....	26
Fig 5.4	Roll angle of ship "A" using PID controller.....	27
Fig 5.5	Roll angle of ship "A" using NN controller.....	27
Fig 5.6	Roll angle of ship "B" using PID controller.....	28
Fig 5.7	Roll angle of ship "B" using NN controller.....	28
Fig 5.8	Roll angle of ship "C" using PID controller.....	29
Fig 5.9	Roll angle of ship "C" using NN controller.....	29
Fig 5.10	Training of NN controller using 2 inputs and 1 target.....	30
Fig 5.11	Ship's roll control using NN controller with 2 inputs.....	31
Fig 5.12	Roll angle of ship "A" using 2-input NN controller.....	31
Fig 5.13	Roll angle of ship "B" using 2-input NN controller.....	31
Fig 5.14	Roll angle of ship "C" using 2-input NN controller	32
Fig 5.15	Training of NN controller using 2 inputs and 1 target.....	32
Fig 5.16	Ship's roll control using NN controller with 3 inputs.....	33
Fig 5.17	Roll angle of ship "A" using 3-input NN controller.....	33
Fig 5.18	Roll angle of ship "B" using 3-input NN controller.....	34
Fig 5.19	Roll angle of ship "C" using 3-input NN controller.....	34
Fig 5.20	RSR roll angle with different number of hidden neurons in NN.....	36

Fig 5.21 Roll angle of ship "A" using 2-input NN controller with 25 hidden neuron	37
Fig 5.22 Roll angle of ship "B" using 2-input NN controller with 25 hidden neurons.....	37
Fig 5.23 Roll angle of ship "C" using 2-input NN controller with 25 hidden neurons.....	38
Fig 6.1 Cut section of a stabilizer and its auxiliary machinery.....	40
Fig 6.2 Figure showing impractical fin angles considered by a researcher.....	41
Fig 6.3 Block Diagram of the system controlled by PID controller with saturation.....	41
Fig 6.4 Roll angles of ship A,B & C using PID controller with saturation limits....	42
Fig 6.5 Block Diagram of the Ship's roll control by NN controller with saturation.....	43
Fig 6.6 Roll angle of ship A,B&C using NN controller with saturation limits.....	44
Fig. 7.1 Output fuzzy set with Gaussian membership functions.....	46
Fig 7.2 Control surface of 1-input FLC with 5 rules.....	46
Fig 7.3 Ship's roll control using FLC with 2 inputs.....	47
Fig 7.4 Control surface of FLC with equal sized Gaussian MFs and 125 rules.....	50
Fig 7.5 Ship's response (A) using FLC with saturation limits and equal sized Gaussian MFs	50
Fig 7.6 Ship's response (B) using FLC with saturation limits and equal sized Gaussian MFs.....	51
Fig 7.7 Ship's response (C) using FLC with saturation limits and equal sized Gaussian MFs.....	51
Fig 7.8 Control surface of FLC with equal sized Gaussian MFs and 25 rules.....	52
Fig 7.9 Fuzzy set with different sized Gaussian MFs intersecting at 25% peak height.....	55
Fig 7.10 Figure showing MFs of various sizes but representing equal no. of PID samples.....	55
Fig 7.11 Fuzzy set of Input-2 with different sized MFs.....	55

Fig 7.12 Fuzzy set of Output with different sized MFs.....	56
Fig 7.13 Control surface for FLC with different sized Gaussian MFs and 125 rules.....	58
Fig 7.14 Control surface for FLC with different sized Gaussian MFs and 25 rules.....	59
Fig 7.15 Fuzzy sets of Input-1,2 and Output of FLC with different sized triangular MFs.....	62
Fig 7.16 Control surface for FLC with different sized triangular MFs and 125 rules.....	63
Fig 8.1 Graphical representation of particle shifting in PSO.....	65
Fig 8.2 Block diagram of the system with saturated FLC and gains.....	66

LIST OF TABLES

Table 1.1	Types of Stabilisers and Principle used.....	2
Table 4.1.	Transfer functions of 3 different stability conditions of the ship.....	21
Table 5.1.	Roll angle(RMS) comparison between PID and NN controllers.....	29
Table 5.2.	Roll angle(RSR) comparison between PID and NN controllers.....	30
Table 5.3.	Roll angle(RMS) comparison between NN controllers with different number of inputs.....	34
Table 5.4.	Roll angle(RSR) comparison between NN controllers with different number of inputs.....	35
Table 5.5.	Roll angle(RMR) comparison between NN controllers with different number of hidden neurons.....	35
Table 5.6.	Roll angle(RSR) comparison between NN controllers with different number of hidden neurons.....	36
Table 5.7.	Roll angle(RMS) comparison between PID and NN controller with 25 hidden neurons.....	38
Table 5.8.	Roll angle(RSR) comparison between PID and NN controller with 25 hidden neurons.....	38
Table 6.1.	Ship's roll angle using PID and NN controllers with saturation.....	43
Table 7.1.	Roll angle(RMS) comparison between various type of fuzzy sets.....	46
Table 7.2.	PID signals used for FLC design.....	47
Table 7.3.	Grouping of PID database for FLC rules creation.....	48
Table 7.4.	Fuzzy rules(25) of FLC with equal sized Gaussian MFs.....	52
Table 7.5.	Ship's roll angle (RMS) using various FLCs with equal sized Gaussian MFs.....	52
Table 7.6.	Six limit points defining five ranges of various fuzzy sets.....	54
Table 7.7.	Parameters of different sized Gaussian MFs.....	54

Table 7.8. Grouping of PID database for rules creation of FLC with different sized MFs	56
Table 7.9. Fuzzy rules(25) of FLC with different sized Gaussian MFs	59
Table 7.10 Ship's roll angle (RMS) using various FLCs with different sized Gaussian MFs.....	59
Table 7.11. RMS of Ship's roll using FLC with zero-centered and different sized MFs.....	60
Table 7.12. Coordinates of the different sized triangular MFs.....	61
Table 7.13. Coordinates of the zero-centered and different sized triangular MFs....	63
Table 7.14. Ship's roll angle (RMS) using various good performing FLCs	64
Table 8.1. Optimized Ship's roll angle with various particle ranges of PSO.....	67
Table 8.2. Optimised Ship's roll angle with different number of particle used in PSO.....	67
Table 9.1. Roll angle comparison between finalised PID, NN and fuzzy logic controllers.....	69
Table 9.2. Roll angle(RMS) comparison between finalised PID, NN and fuzzy logic controllers.....	70
Table 9.3. Roll angle(RSR) comparison between finalised PID, NN and fuzzy logic controllers.....	70
Table 9.4. Roll frequency (per min) comparison between finalised PID, NN and FLC.....	71

LIST OF ABBREVIATIONS

PID	Proportional Integral derivative
GMt	Transverse Metacentric height of a ship
NN	Neural Network
FLC	Fuzzy logic controller
MF	Membership function
MFs	Membership functions
RMS	Root mean square
RSR	Reduction of Statistics of Roll
Mux	Multiplexer
Sat	Saturation

Chapter 1

Introduction

1.1 Background

In the marine world, various types of ships exist which have different and wide variety of roles. In spite of the diversity in their roles, a common problem faced by most of the ships at sea is transverse rolling motion. Roll motion, in particular, affects ship performance in the following ways[1]:

- Transverse roll motion induce interruptions in the tasks performed by the crew. This increases the amount of time required to complete the missions, and in some cases may even prevent the crew from performing tasks at all. This can render naval ships inoperable.
- Roll motion at locations away from the ship's centre line can contribute to the development of seasickness in the crew and passengers, which affects performance by reducing comfort.
- Roll motions may produce cargo damage, *e.g.* on soft loads such as fruit especially in cargo ships.
- Large roll angles limit the capability to handle equipment on board. This is important for naval vessels performing weapon operations, launching or recovering systems, and sonar operation.

Ship roll stabilization refers to the reduction of the undesired ship roll motion induced by the waves. A stabilizer or ship roll stabilization system is used to reduce ship roll motion induced by the disturbances especially sea waves.



Fig1.1 Devastating effects of ship's roll[5]

1.2 Ship Roll Stabilization Techniques

The first elements leading to good ship roll stabilization (SRS) are careful hull design and load distribution. It was shown by Froude, in his seminal paper *On the rolling of ships* [1], that it is not the height of the waves, but the steepness/slope of the waves what excites the rolling motion of a ship. He further commented that since short waves appear to be steeper than long waves, there is, then, no advantage in trying to reduce the natural roll period of the vessel. Instead, this period should be extended as much as possible so as to avoid synchronization with the wave excitation frequency.

Despite good efforts to extend the natural period of the vessel, it is inevitable that wave loads will excite roll for some sailing conditions. In addition, the damping of the hull may not be sufficient to attenuate roll motion to the desired levels. For these reasons, the vessel is often equipped with roll reduction systems. As commented by Chadwick[2], if one looks at the patent registers, there have been a large number of proposals from which only a few passed the stage of a prototype. Further, he makes the observation that all stabilisers depend on the motion of mass; thus, they can be classified as follows:

1.3 Types of Stabilisers. There exist various types of stabilization techniques which use different principles to reduce the ship's roll. Types of stabilisers are listed below:

Table 1.1. Types of Stabilisers and Principle used

<u>Sl No</u>	<u>Stabilization technique</u>	<u>Principle used</u>
(a)	Gyroscopes	Acceleration of Internal Solid mass
(b)	Bilge keels	Acceleration of External Fluid mass
(c)	Fins	Acceleration of External Fluid mass
(d)	Rudder	Acceleration of External Fluid mass
(e)	Motion of weights	Displacement of Internal Solid mass
(f)	Anti-roll tanks	Displacement of Internal Fluid mass

1.3.1 Gyroscopes

The gyroscope type of stabiliser consists of using the gyroscopic effects of a large rotating wheel to generate a reducing moment. The use of gyroscopic effects was

proposed as a method to eliminate roll, rather than to reduce it. This method is not currently in use mainly due to heavy weight of the equipment. A sample photo is shown below:

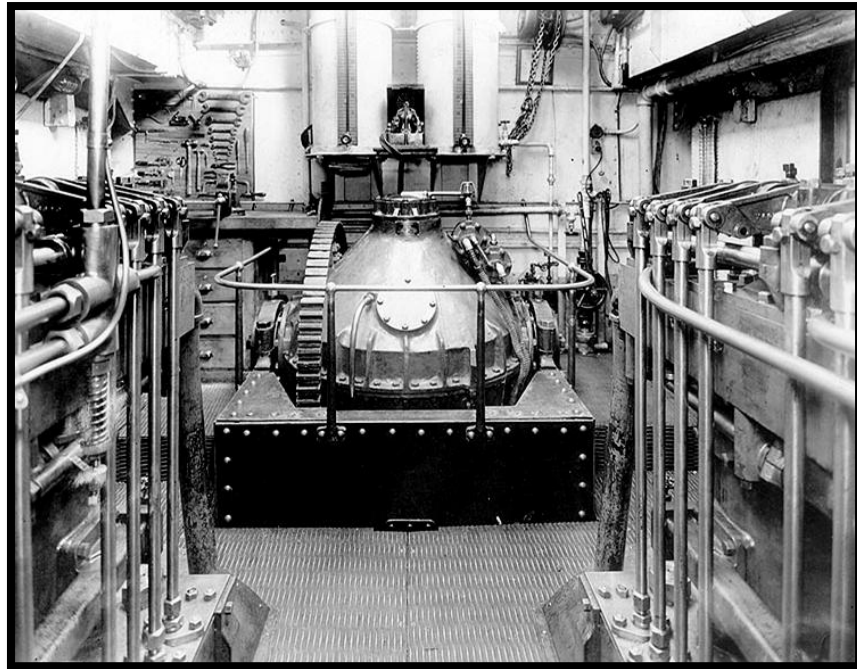


Fig 1.2 Gyro stabiliser installed on USS Aramis[63]

1.3.2 Bilge Keels

Bilge keels are the simplest form of stabiliser. These are long narrow keels mounted on the turn of the bilge. Figure 1.2 shows a conventional arrangement. The idea of using bilge keels was apparently put forward by Froude in the mid-19th century. Bilge keels increase the hull damping by generating drag forces that act perpendicular to the keels and oppose the roll motion. In this way, the kinetic energy associated with roll is converted to fluid kinetic energy by viscous effects (shed vortices). The main advantages of bilge keels are the following:

- Relatively effective source of damping, especially at low speeds. The performance is in the range of 10–20% of roll angle reduction [1].
- Low maintenance; no more than that normally done to the hull.
- No occupied space and no significant increase of ship dead weight.
- Low price and easy installation

Some disadvantages of bilge keels are indicated as follows:

- Increase of hull resistance in calm water conditions (when roll reduction is not necessary.) Although this is alleviated by careful alignment with the hull streamlines, the increase of resistance in calm water can still be significant.
- Not all ships can be fitted with bilge keels. For example, they could be a potential problem for fishing vessels deploying nets, and are very easily damaged in ice-breakers.

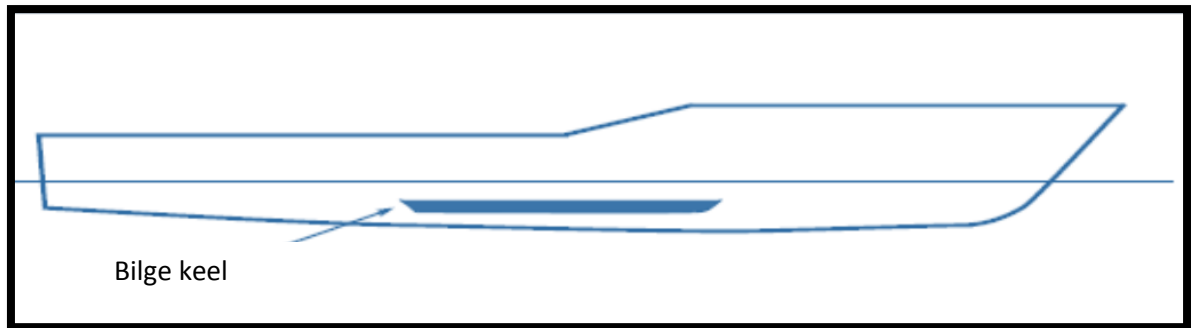


Fig 1.3 Bilge Keel for Ship Stabilization[63]

1.3.3 Anti-rolling Tanks

The most widely used anti-roll tank is the U-tube tank, originally developed by Frahm in 1911. This type of tank is composed of two reservoirs, located one on port and one on starboard, connected at the bottom by a duct as shown in Figure 1.3. The principle of operation of anti-roll tanks is that as the ship rolls, the fluid inside the tank (usually water) moves with the same period the ship moves, but lagging a quarter of period behind the rolling of the vessel. This way, the weight of the mass of fluid produces a moment that opposes the roll motion. This moment attains its maximum values when the ship passes through its vertical position[3, 4].



Fig 1.4 . Cut section of Anti-Roll tank [5]

The main advantages of anti-roll tanks are the following:

- Medium to high performance. This has been estimated to be in the range of 20–70% of roll reduction
- Performance is independent of the operation speed of the vessel. This makes them the preferred option for vessels that spend a large amount of time operating at low or zero speed (*e.g.* fishing vessels).
- Low maintenance.
- Relative cost of these stabilisers is in the middle range.
- By incorporating appropriate additional features, the tank can also serve as an anti-heeling device to compensate for uneven distribution of load.

Some disadvantages of anti-roll tanks are indicated as follows:

- Reduction of deadweight; estimated to be in the range of 1–4% of displacement.
- Occupy large spaces.
- Affect the stability of the vessel due to free-surface effects. When a tank is not completely full and there is space for the water to move (free surface), there is a loss of transverse meta-centric height due to the motion of the centre of gravity. This should be accounted for to avoid ship stability problems.

1.3.4 Active Fin Stabilisers

Fin stabilisers consist of a pair of hydrofoils mounted on rotatable stocks at the turn of the bilge located about amidships as shown in Figure 1.5. As the ship rolls, this motion is fed back to the control system, which commands the actuator to modify the angle of incidence of the fins. Once there is an angle between the flow and the fin, hydrodynamic lift is generated, and a stabilising moment is obtained as a result of the generated lift and the location of the fins on the hull. As in any lifting device, the amount of lift, and hence the generated moment, depend on the vessel speed. At speeds higher than 10-15 knot, active fins are the most effective stabiliser.



Fig. 1.5. Typical fin stabiliser arrangement[6]

The main advantages of fin stabilisers are appended below:

- High performance, normally estimated in the range of 50–90% of roll reduction.
- Relatively easy control system design.

Some disadvantages of fin stabilisers are indicated as follows:

- Ineffective at low speeds.
- Costly maintenance.
- Need for control system with sensors and powerful hydraulic actuators.
- Easily damaged and with high risk of grounding when operating in shallow water or coming alongside other ships.
- Increased hull resistance when in use. Large-span fins are not usually viable (particularly if they are not retractable); thus, a small lift to drag ratio results from the usually low aspect ratio characteristics of the commonly employed fins. A rough estimate of speed loss due to fin activity is 10%[7].
- Increased resistance in calm water if they are not retractable. Retractable fins are more expensive and may require large spaces.
- Possibility of introducing underwater noise affecting sonar systems.
- Most expensive.

1.3.5 Rudder Roll Stabilization (RRS)

Rudder roll stabilization is a technique based on the fact that the rudder is located aft and also below the centre of gravity of the vessel, and thus the rudder imparts not only yaw but also roll moment. RRS is an extra feature of the course autopilot[8]. Most of the drawbacks of conventional active fin stabilisers and anti-roll tanks are overcome by RRS. Provided the speed of the ship and the **rudder rate are sufficiently high**, this technique can be applied to different ship types: small and large naval vessels, patrol (coastguard) vessels, ferries and some Ro-Ro vessels[1]. A sample photo of a ship's rudder is shown below:



Fig 1.6 Rudders of a ship[9]

The main advantages of RRS are the following:

- Medium to high performance. This can be in the range of 50-75% of roll reduction
- Relatively inexpensive.
- No resistance in calm water conditions.
- No large spaces required.
- Can be combined with other stabilisers to achieve higher performance.

Some disadvantages of RRS are indicated below:

- Ineffective at low speeds. Nevertheless, this can be higher than that of fins because the rudders are located in the race of the propellers; and thus, operate in higher speed flows than fins.
- Drag is produced when in use. Nevertheless, this can be less than the drag of fin stabilisers, provided ship turning is prevented.
- Rudder machinery up-grade may be needed to achieve high performance through faster rudder motion.
- Need sophisticated control systems to extend the good performance to different sailing conditions.

Out of these major six types of stabilisation techniques mentioned above, usage of (active) fin stabilisers is most popular in the modern day ships. The dissertation report will continue on the control of **active-fin stabilisers**.

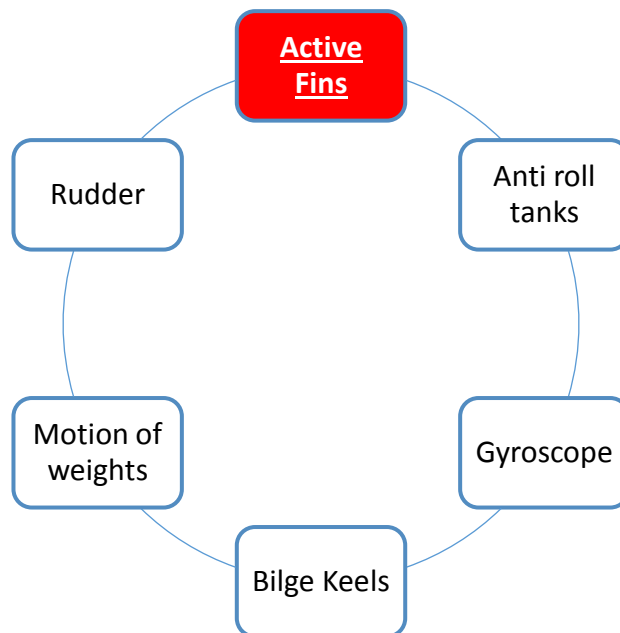


Fig 1.7 Types of Stabilizers

Chapter 2

Active Fin Stabilisers

2.1 Principle of Operation. The stabilizers operate on the simple principle of generation of hydrodynamic forces by relative movement of water over the submerged stabilizer fins. This is similar to aircrafts which go up because of the lift produced by the wings. The fins are turned clockwise or anticlockwise (Figure 2.1) in the (relative) moving stream of water to generate a lift so as to counter the external dynamic heeling forces of waves or winds. The two fins, fitted on the starboard(right) and port(left) side always work in tandem but in opposite directions. The magnitude of the turning angle through which the fins should turn is decided by the ships speed (relative speed of water over the fin), and the rolling rate of the ship.

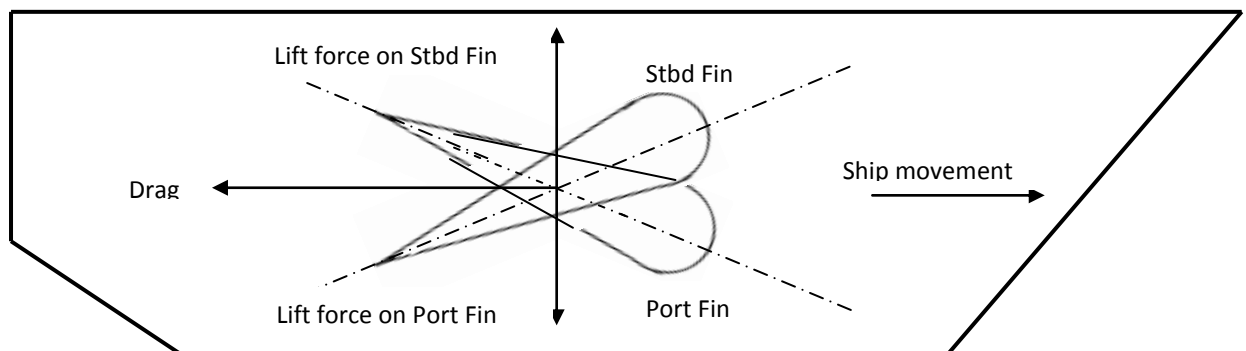


Fig 2.1 Hydrodynamic Forces acting on Stabilizer Fins

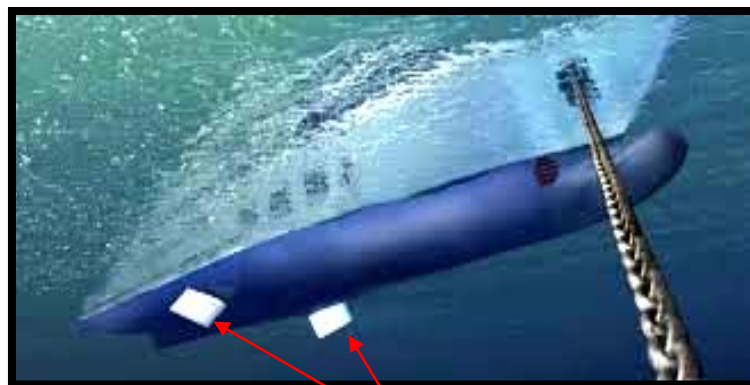


Fig 2.2 Photo showing relatively small size of stabilizers below waterline[24]

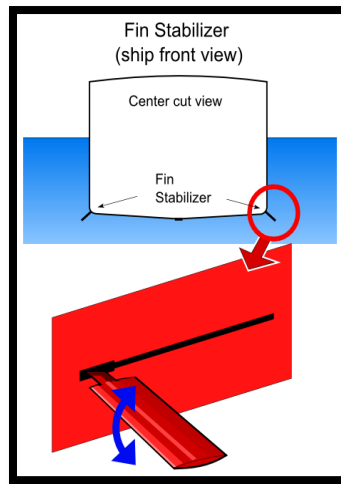


Fig 2.3 Front and side view of Stabilizer[25]

2.2 Direction of Fin Movement. The direction of fins movement is opposite in comparison to each other and the same is shown in Fig 2.4 (courtesy: www.dieselship.com) The direction of both the fins change when ship rolls to the other direction. The stabilizer may be used not just to reduce roll of a ship but also to induce/create roll for training and testing purposes.

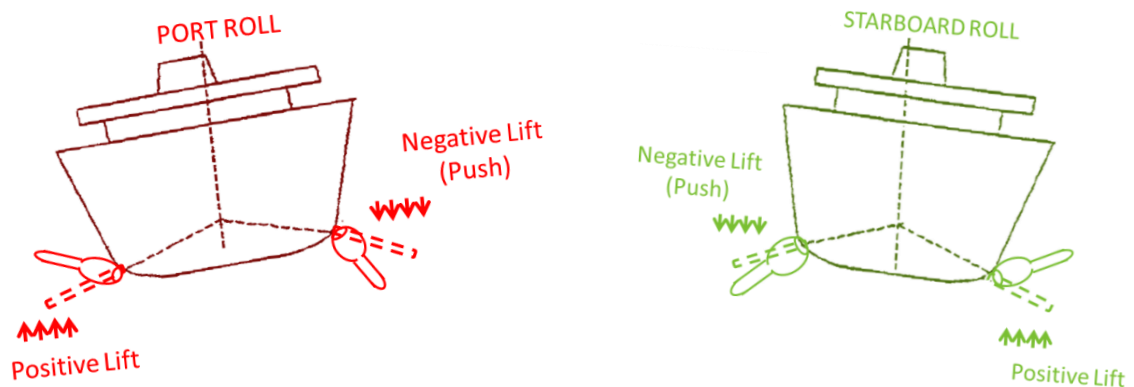


Fig 2.4. Direction of fins motion for both side rolls[3]

Chapter 3

System Modeling

3.1 Various Moments Acting Towards Ship Roll

Rolling motion can be expressed by linear differential equation with constant coefficients. Superposition principle can be applied to analyze ship rolling force under the wave action, using x-axis (ship's heading direction) roll angle ϕ , roll velocity $\dot{\phi}$ and roll acceleration $\ddot{\phi}$ to describe the rigid body roll of the ship movement. We define clockwise positive and anticlockwise negative when we observe from bow to stern. This mathematical modeling starts with the linear theory, assuming that the ship is time-invariant linear system.

Ship rolling force on the sea waves can be divided into the following five kinds of moments:

- (a) **Restoring moment.** This moment tends to get the ship back to its normal equilibrium position due to the lateral difference between center of buoyancy and center of gravity.

$$M(\phi) = -Dh\phi \quad (1)$$

In the above equation, D is displacement(mass*g) of the ship, h is initial stability height (metacentric height GM) and ϕ is the present ship's roll angle.

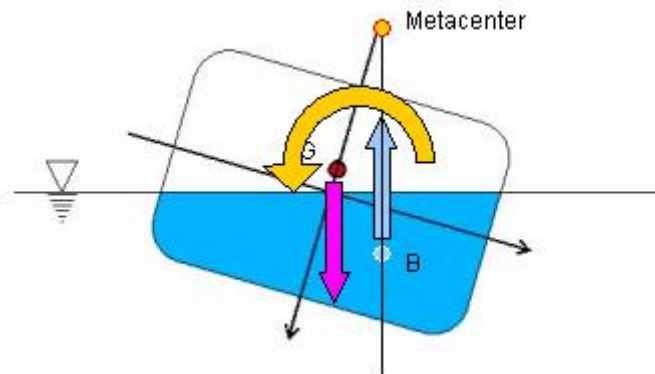


Fig 3.1 Restoring moment is dependent on center of gravity and buoyancy[26]

(b) **Roll damping moment.** This moment resists the motion and is mainly decided by the damping coefficient N_u . This also depends on the surface of the hull. In the equation given below N_u is the damping coefficient.

$$M(\dot{\phi}) = -N_u \dot{\phi} \quad (2)$$

(c) **Inertia moment.** It consists of the inertia moment of the ship and the additional inertia moment.

$$M(\ddot{\phi}) = -(I_{xx} + \Delta I_{xx}) \ddot{\phi} \quad (3)$$

Here ΔI_{xx} is considered to be 10% of the I_{xx} [1]. This accounts for various additional inertia moment acted upon due to the sea water upon the ship's hull from sides.

(d) **Wave disturbance moment.** The wave disturbance is added as a disturbance to the ship's roll movement and is discussed in the later sections of this report.

(e) **Righting moment.** This is the moment created because of the stabilizers fin and is dependent on the equivalent wave angle of the stabiliser fin α_f .

$$M(\phi) = -Dh\alpha_f \quad (4)$$



Fig 3.2 Righting moment created by stabilizers

3.2 Mathematical model of ship dynamics. Considering various ship moments in regular waves as explained above, ship equilibrium conditions are that all the moments add up to close to zero. So the mathematical model of the linear rolling motion of the ship is:

$$(I_{xx} + \Delta I_{xx})\ddot{\phi} + 2N_u\dot{\phi} + Dh\phi - Dh\alpha = 0 \quad (5)$$

so, it can be re-written as shown below:

$$(I_{xx} + \Delta I_{xx})\ddot{\phi} + 2N_u\dot{\phi} + Dh\phi = Dh\alpha \quad (6)$$

Here, the moments due to sway motion and yaw motion are neglected in a three degree of freedom model of a ship (roll, sway and yaw motions) as their values are much smaller in comparison to the other terms. The actual three degree of freedom model of a ship otherwise would actually been as shown below[23]:

$$(I_{xx} + \Delta I_{xx})\ddot{\phi} + 2N_u\dot{\phi} + 2N_v v + 2N_{\dot{\psi}}\dot{\psi} + Dh\phi = Dh\alpha_e + K_s s \quad (7)$$

where $N_v, N_{\dot{\psi}}$ are the damping coefficients because of sway velocity and yaw velocity respectively; $K_s s$ is the moment caused due to the sea waves which is separately added in the model after the ship's dynamics.

Equation (6) is called as the Conolly linear rolling equation that is widely used in the practical marine engineering[18]. It describes the ship linear rolling model. It has been widely applied in control system of the ship equipped with damping device. As mention before, I_{xx} is rolling moment of inertia; ΔI_{xx} is the additional moment inertia; N_u is the roll damping coefficient; D is the displacement of ship; h is the initial stability height; ϕ is the roll angle; α is effective wave angle of the stabilizer fin .

By applying Laplace transformation of equation(6) mentioned above with initial conditions as $\ddot{\phi}(0) = \dot{\phi}(0) = \phi(0) = 0$ we get,

$$\frac{\phi(s)}{\alpha(s)} = \frac{-Dh}{(I_{xx} + \Delta I_{xx})s^2 + 2N_u s + Dh} \quad (8)$$

Rearranging, we get the ship roll motion transfer function as,

$$G(s) = \frac{\phi(s)}{\alpha(s)} = \frac{-1}{\frac{(I_{xx} + \Delta I)}{Dh} s^2 + \frac{2N_u}{Dh} s + 1} \quad (9)$$

This can also be expressed as a standard second order transfer function as mentioned below:

$$G(s) = \frac{\phi_s(s)}{\alpha_e(s)} = \frac{1}{T_\phi^2 s^2 + 2T_\phi \xi_\phi s + 1} \quad (10)$$

here, relevant parameters are

$$T_\phi = \sqrt{\frac{I_{xx} + \Delta I_{xx}}{Dh}}$$

$$\xi_\phi = \frac{N_u}{\sqrt{Dh(I_{xx} + \Delta I_{xx})}}$$

The relevant parameters of NO.32 Denmark fisheries ship are[18]:

$$I_{xx} + \Delta I_{xx} = 1.76 \cdot 10^6 \text{ kgm}^2, T_\phi = 1.27323, \xi_\phi = 0.1846, h = 1.012 \text{ m}, N_u = 2564410.3 \text{ kgm}^2/\text{s}$$

These parameters are taken into the Conolly rolling equation to get the following equation at speed of 18 miles per hour:

$$G(s) = \frac{1}{1.62s^2 + 0.47s + 1} \quad (12)$$

3.3 Wave Disturbance Model

The wave disturbance or the roll motion affected because of the sea waves is actually a combination of infinite number of sin waves with different wave lengths and amplitude. In many literatures, its common to see that the wave disturbance is considered as a sin wave or a summation of few sine waves with different parameters. However, the practical disturbance caused due to the sea waves is far from this approximation. A closest model of the same as an output disturbance can be achieved by passing a white noise through a second order shaping filter defined by[2]

$$H(s) = \frac{K_w s}{s^2 + 2\xi\omega_e s + \omega_e^2} \quad (13)$$

where K_w is a coefficient that can be adjusted to represent wave strength effect ; ξ is a damping ratio and ω_e is the encounter frequency. Typically, ξ is between 0.05 to 0.1 and ω_e is between 0.3 to 1.3 rad/sec. In the simulation study, ξ is set to 0.075, ω_e is 0.4 and K_w is 10, which result in a narrow band type of disturbance[4]. To a first order approximation, wave motions are linear and the hull response can be

obtained as a superposition of the wave induced motion and that created by fin activity. In the following computations, the damping ratio ξ is set to 0.075, the encounter frequency ω_e is set to 0.4 rad/sec and the wave strength factor K_w is set to 10, which will give a wave-induced roll motion within 15 deg on either side. The wave shaping filter employed in the simulation study is then given by

$$H(s) = \frac{10s}{s^2 + 0.06s + 0.16} \quad (14)$$

The roll motion induced by using the above wave model is plotted using MATLAB software as shown below:

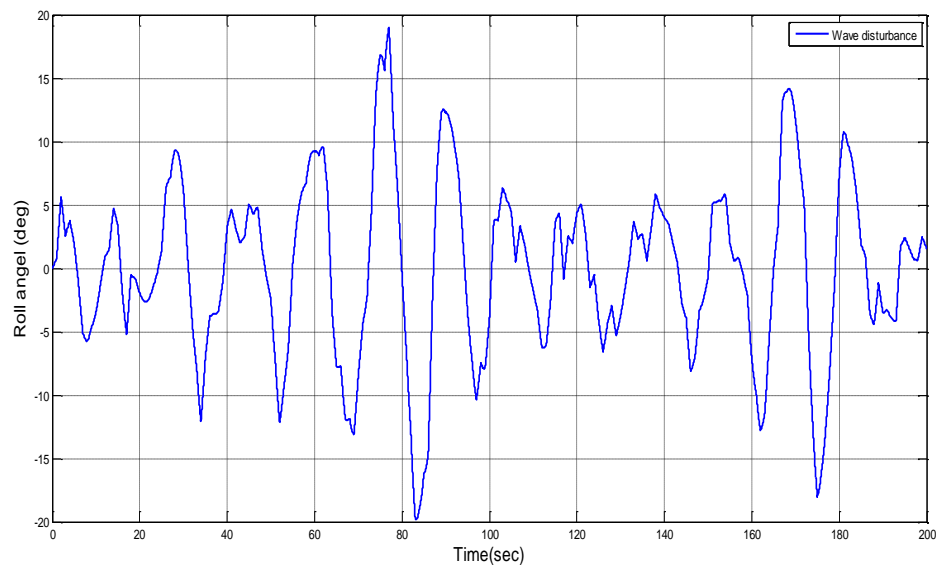


Fig 3.3 Wave disturbance considered for ship's roll motion

3.4 Control System Model

The block diagram of the ship's roll motion control is designed as shown in Fig 3.4:

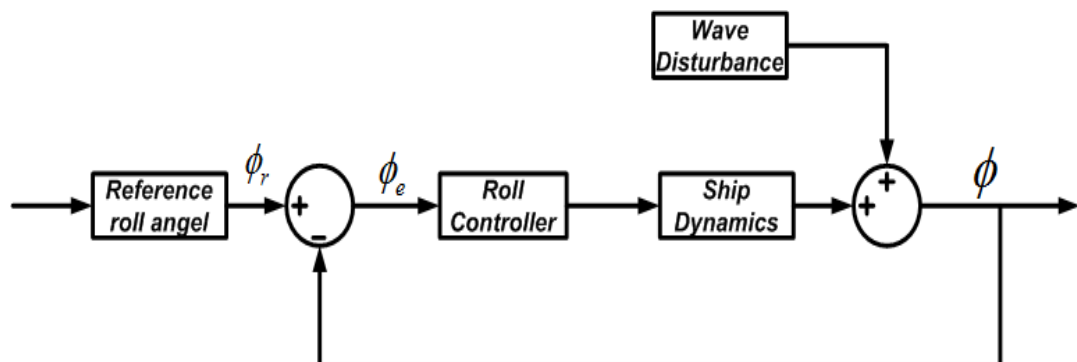


Fig 3.4 Block diagram of the ship's roll control system

The "Roll Controller" in the above block diagram refers to the controller of the plant/ship which can be any suitable type of controller like PID controller or neural network controller. The "Ship Dynamics" was already discussed in the previous section through the mathematical modeling of the plant/ship. The "Wave Disturbance" is the white noise passed through the filter as discussed before so as to create a natural roll disturbance which is close to the natural sea waves disturbing the ship's transverse roll motion. This disturbance is added to the output of the ship dynamics which is the ship's roll angle ϕ . Since both are linear in nature, they are summed and the output is the final roll angle of the ship which is fed back to the controller (negative feedback). The reference signal ϕ_r is 'zero' as the desired output is 'zero' degrees of ship's roll. The same can be a non-zero value/variable when a roll is desired to be induced in the system for training or testing purposes. So, in the case of roll stabilization the reference signal is always 'zero'. The error signal is the difference of the feedback signal and the reference signal. Now based on the output of roll controller, the stabiliser fin angle is controlled and the ship's roll is stabilized in spite of the large wave disturbances.

Chapter 4

PID Controller And Related Problems

4.1 PID Controller. As proportional–integral–derivative controller (PID controller) is a control loop feedback mechanism (controller) which is most commonly used in industrial control applications [12, 27], the same was initially designed for the ship roll control. It is known that PID controller continuously calculates an error value (ϕ_e) as the difference between a measured process variable (ϕ , ship's roll angle) and a desired set point (ϕ_r , the value of the same is 'zero' in this case for roll stabilization). The controller attempts to minimize the error over time by adjustment of a control variable, to a new value determined by a weighted sum:

$$u(t) = K_p \phi_e(t) + K_i \int_0^t \phi_e(t) dt + K_d \frac{d\phi_e(t)}{dt} \quad (15)$$

and $G(s)$, the transfer function of the controller is:

$$G_c(s) = K_p \left(1 + \frac{1}{T_i s} + T_d s \right) \quad (16)$$

where K_p , K_i and K_d , all non-negative, denote the coefficients for the proportional, integral and derivative terms, respectively. Ziegler-Nichols tuning rules were used to tune the PID controller of the ship/plant wherein the value of K_p , K_i ($=1/T_i$) and K_d ($=T_d$) are determined by the following formulae:

$$K_p = 0.6 K_{cr}$$

$$T_i = 0.5 * P_{cr}$$

$$T_d = 0.125 * P_{cr}$$

Applying the above formulae to start with and and by further fine-tuning the PID controller, the final output of the model or the ship's roll angle with time is plotted using MATLAB software and is shown in Fig 4.1:

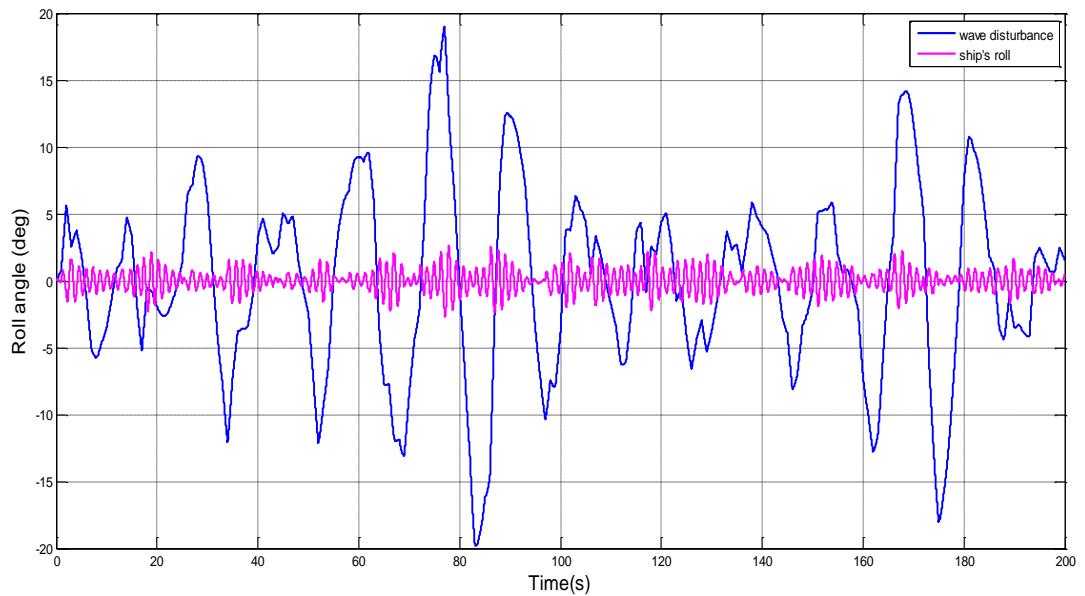


Fig 4.1 Ship's response with the tuned PID controller

4.2 Initial Analysis. The RMS value of the ships roll without the controller in the above plot was calculated to be 6.8798 degrees and that with the PID controller is 0.82 degrees. The value is moderately good and values below 2 degrees are acceptable conditions for a normal ship but with no value reaching a roll angle more than 5 degrees.

4.3 Parameter Variations / Perturbations in the system:

There exists various factors which change the transfer function of the ship. The various reasons for change of parameters are explained below:

4.3.1 Ship's Displacement/Weight.

- Fuel and other liquid tanks constitute a major portion of the weight of the ship which varies gradually with time and can sometimes contribute up to 30% of total weight.

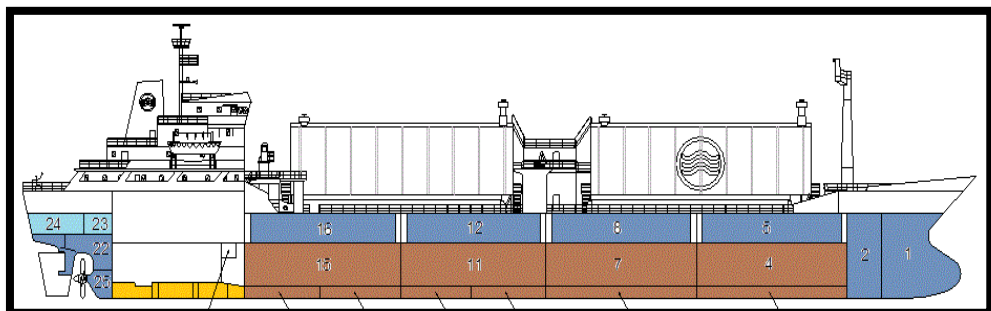


Fig. 4.2 Large portion of ship's weight is its fuel (coloured brown)[66]

- In naval vessels, missiles can weight up to 3 tonnes/missile[28] or even more and each firing of the same can change the ship's weight to a great extant.



Fig 4.3 Ship version of Brahmos missile weighing 3000 kgs [29]

- Fishing vessels have a lot of weight fluctuations based on their catch

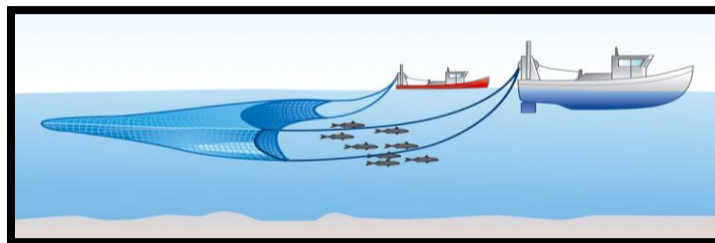


Fig 4.4 Fishing trawlers with heavy fishing nets[61]



Fig 4.5 Photo depicting the large size of fishing nets[61]

- Cargo ships also have a lot of weight changes due to the change of cargo they carry. It includes loading and unloading of cargo.

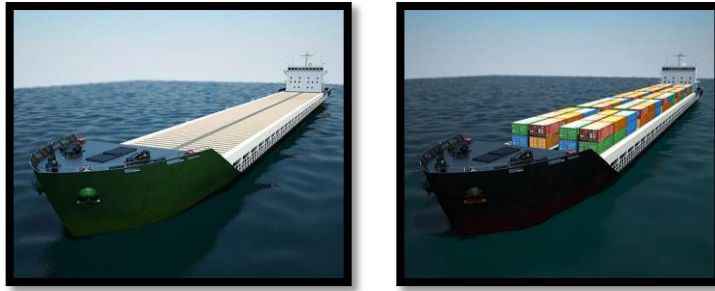


Fig 4.6 Cargo ship with and without its large cargo[60]

4.3.2 Meta centric height

Because of rolling, the liquids in the semi filled tanks shift their relative position in the tanks leading to change of center of gravity/mass of the ship. This leads to change of center of gravity. Also, with change in ship's weight as explained above, centre of buoyancy changes. Due to the change in center of buoyancy and center of gravity, metacentric height can change which is a very important factor shaping the ship's transfer function.

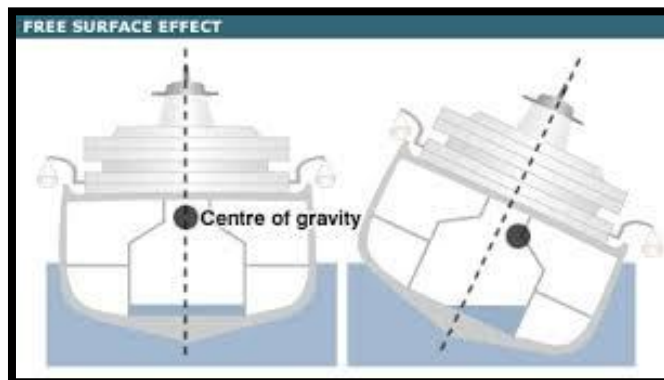


Fig 4.7 Change in center of gravity due to free surface effect[30]

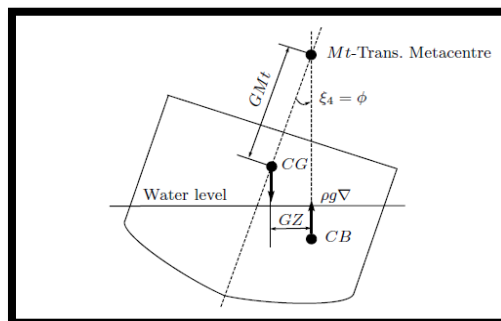


Fig 4.8 Metacentric height (GMt) of a ship[3]

4.3.3 Coefficients

With time, the ship's hull corrodes steadily and loses its smoothness. Apart from the corrosion marine growth on the ships bottom hull surface changes the damping coefficient of the ship and thus leading to a change in the ship's transfer function.



Fig 4.9 Corroded ship's hull[59]



Fig 4.10 Marine growth on ship's bottom surface[58]

So the controlled plant has obvious parameters' uncertainty due to the factors explained above. This effect the coefficients of the ship's transfer function which in the general form of:

$$G(s) = \frac{a}{bs^2 + cs + d} \quad (17)$$

4.4 Three types of ship models. The coefficients a,b,c and d here can vary in the ranges specified below as the parameters of the ship change[18]:

$$a \in [0.528,1.496]; b \in [1.198,2.082];$$

$$c \in [0.295,0.603]; d \in [0.487,1.513].$$

Within the given ranges, we have carefully chosen 3 sets of values to give **three different type of models of the ship** as given below:

Table 4.1. Transfer functions of 3 different stability conditions of the ship

<u>Sl No</u>	<u>Transfer function</u>	<u>Ship's Reference Name</u>	<u>Remarks</u>
(a)	$G(s) = \frac{1}{1.62 s^2 + 0.47 s + 1}$	"A"	Normal condition of ship
(b)	$G(s) = \frac{1.496}{1.198s^2 + 0.603s + 0.487}$	"B"	Highly stable condition of ship
(c)	$G(s) = \frac{1}{2.082s^2 + 0.295s + 1}$	"C"	Less stable condition of ship

Ship's roll angle with time along with the wave disturbance for the ship in all the above 3 cases(A/B/C) is plotted below using MATLAB:

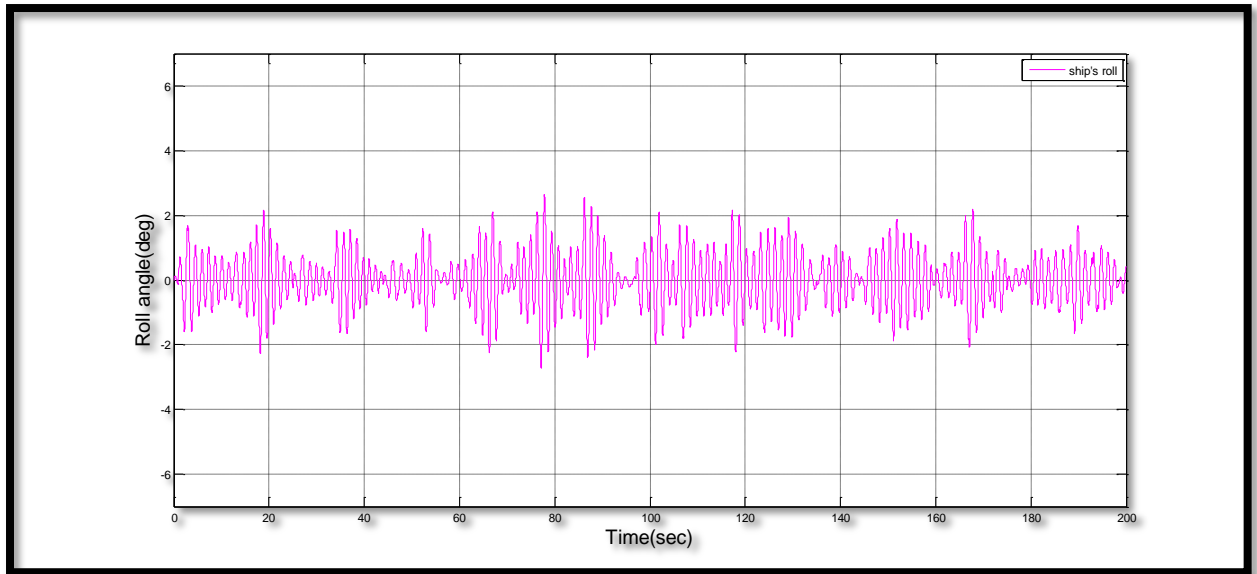


Fig 4.11 Roll angle of ship "A" using PID controller

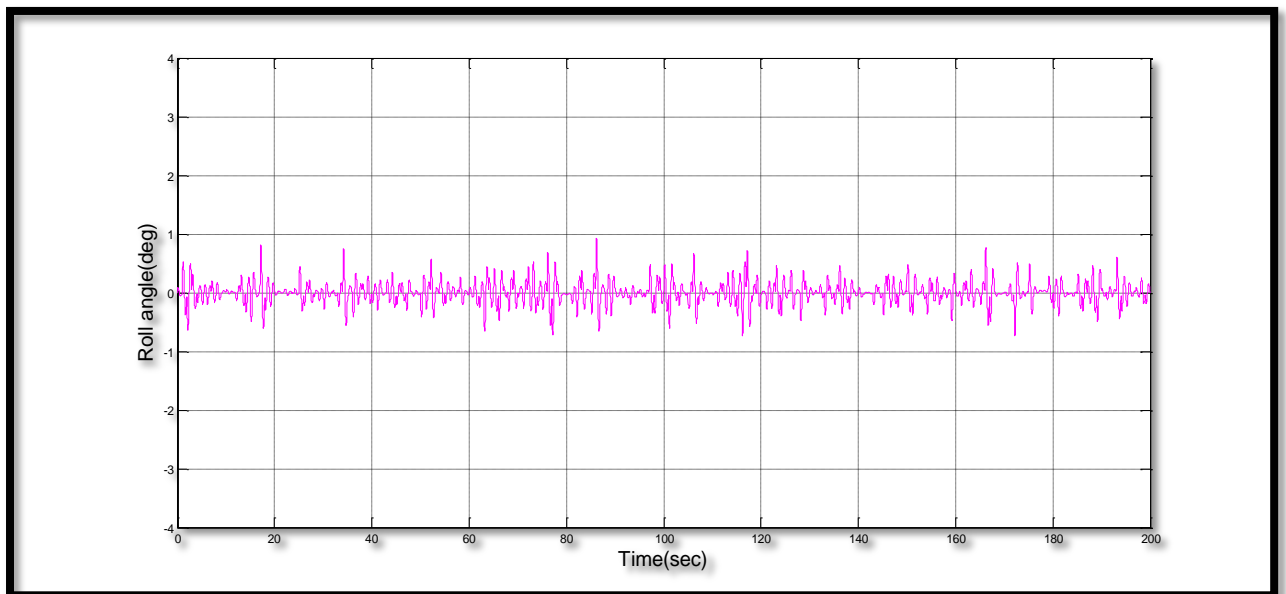


Fig 4.12 Roll angle of ship "B" using PID controller

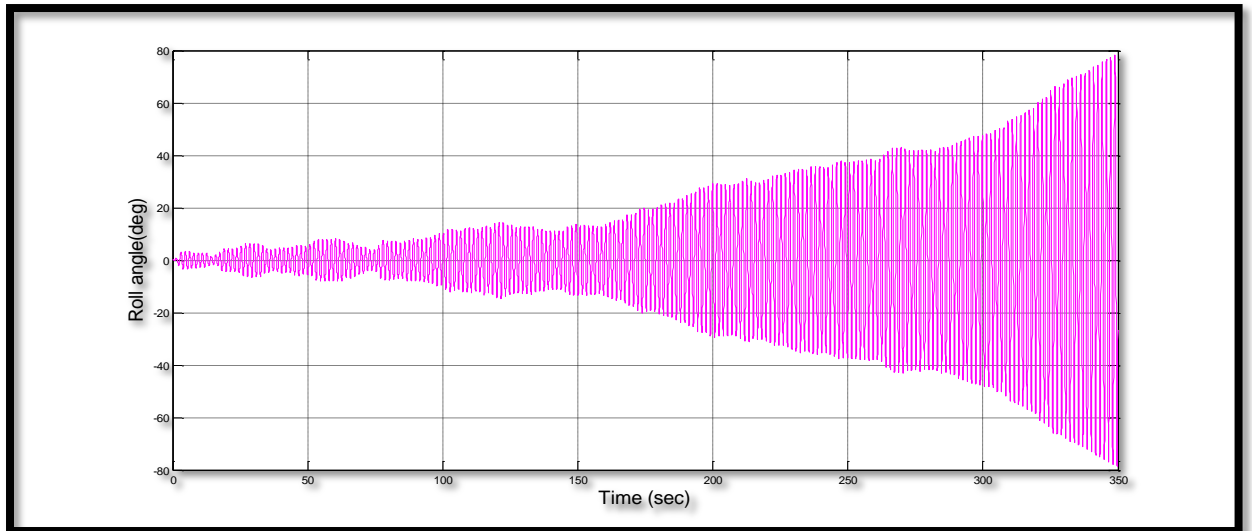


Fig 4.13 Roll angle of ship "C" using PID controller

4.5 Stability curve. A stability gives the restoring moment the ship gets to get back to its upright position because of the shift in centre of gravity and/or centre of buoyancy. The righting moment is plotted for every roll angel of the ship in transverse direction. the positive value indicated a restoring moment which will stabilise the ship. A positive value of righting moment indicates a moment which tends to sink the ship. A sample stability curve for a ship is shown below. The angle of vanishing stability is the angle of roll at which the righting moment stops restoring the roll and adds on to the roll moment in the sinking direction so as to increase the roll angle.

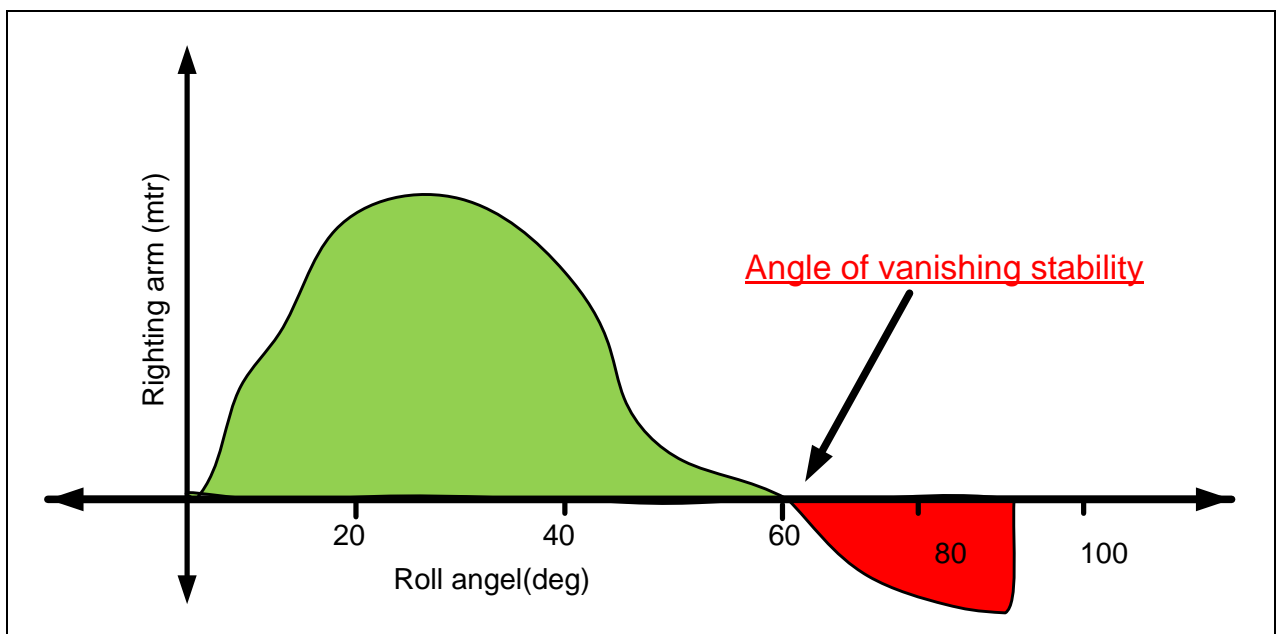


Fig 4.14 A typical stability curve showing righting lever vs. roll angle

From the above stability curve and the ships roll in case C, it is clear that the ship will roll more than 60 degrees at time=320 sec. This is the time when the righting moment or restoring moment will add on to the ship's roll in the same direction and leads to capsizing of the ship.

So, PID controller has such a major disadvantage where in there exists at least one situation(type "C") wherein the **ship sinks** because of the control action which is actually intended for controlling the roll motion.

Chapter 5

Neural Network

5.1 Introduction. Artificial neural network is generally presented as a system of interconnected neurons which exchange messages between each other. The connections have numeric weights that can be tuned based on experience, making neural nets adaptive to inputs and capable of learning. The neural network consists of input, hidden and output layers as shown in Fig 5.1. The network converts the inputs according to the connection weights. These weights are adjusted during the learning process to minimize the sum of the squared errors between the desired output (target) and the network output. Neural networks are particularly effective for predicting events when the networks have a large database of prior examples to draw on[10]. The back-propagation algorithm is the most important algorithm for the supervised training of NN. In this method, error signals are propagated backward through the network on a layer-by-layer basis. The same is used in this section for updating the neural networks.

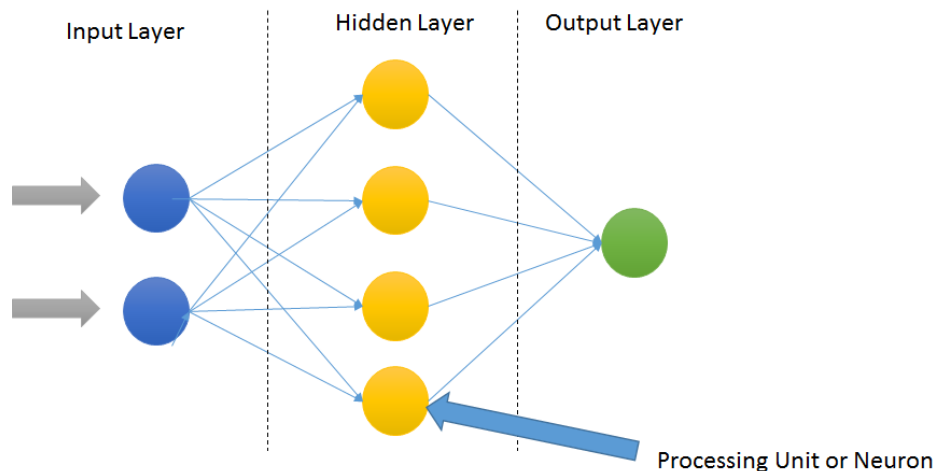


Fig 5.1 A simple neural network

To overcome the disadvantage of the PID controller explained in the previous section especially while considering type "C", a neural network controller has been trained and tested replacing the PID controller.

5.2 Training of NN Controller. As actual data of the practical ships roll is not available for training the ship, the input and output data of the PID controller

(error signal and control signal) which is separately tuned in each of the three cases(A,B,C) are used as input and target **whilst training a neural network** as shown in the below block diagrams. More than **45,000** samples are used to train the NN controller.

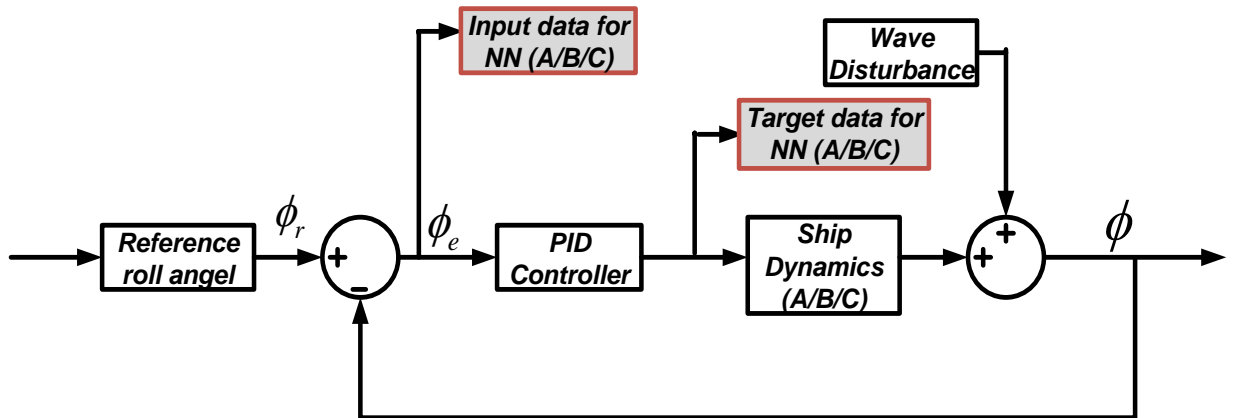


Fig 5.2 Training of NN controller with one input and one target

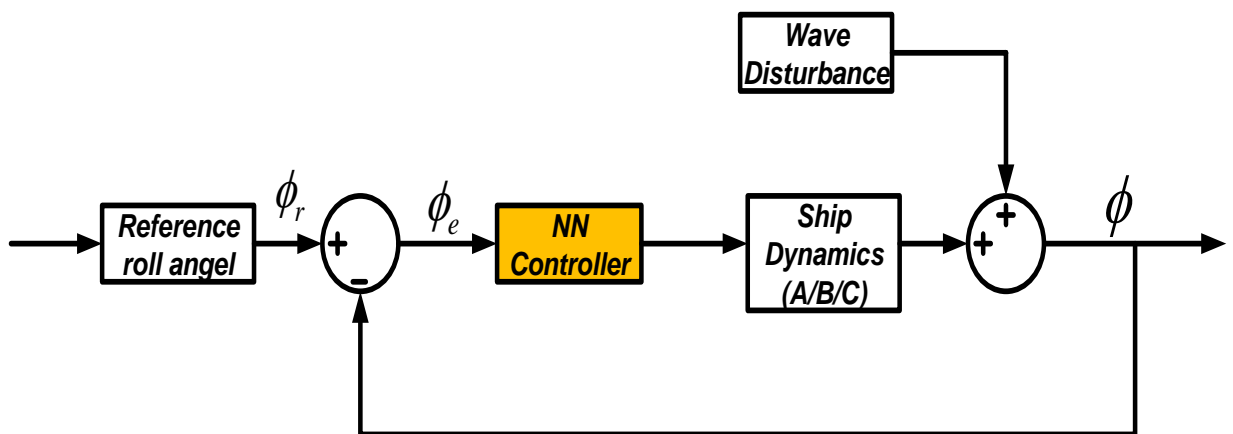


Fig 5.3 Ship's roll control using NN controller

5.3 Performance of NN Controller. The output (ship's roll) of the systems A,B and C with NN controller is plotted as shown below using MATLAB plot:

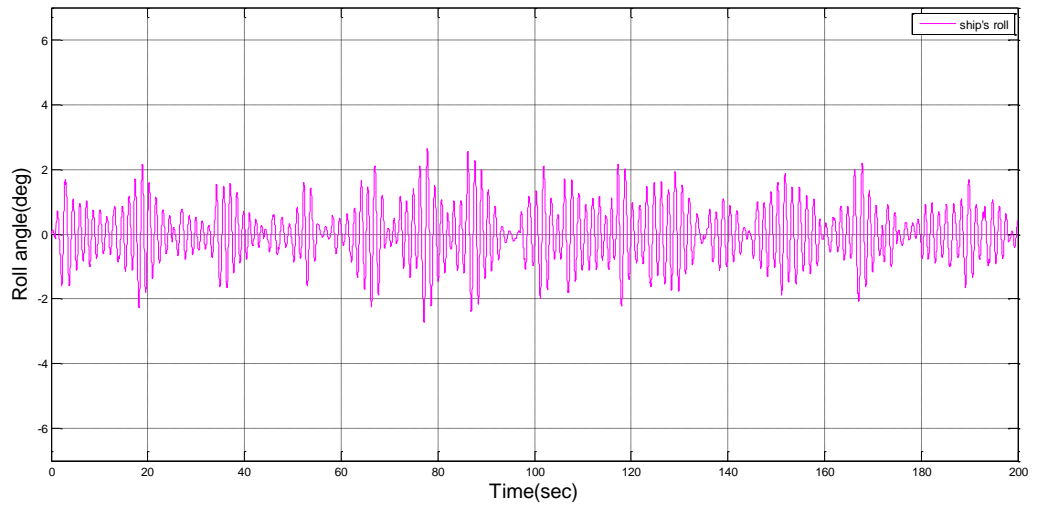


Fig 5.4 Roll angle of ship "A" using PID controller

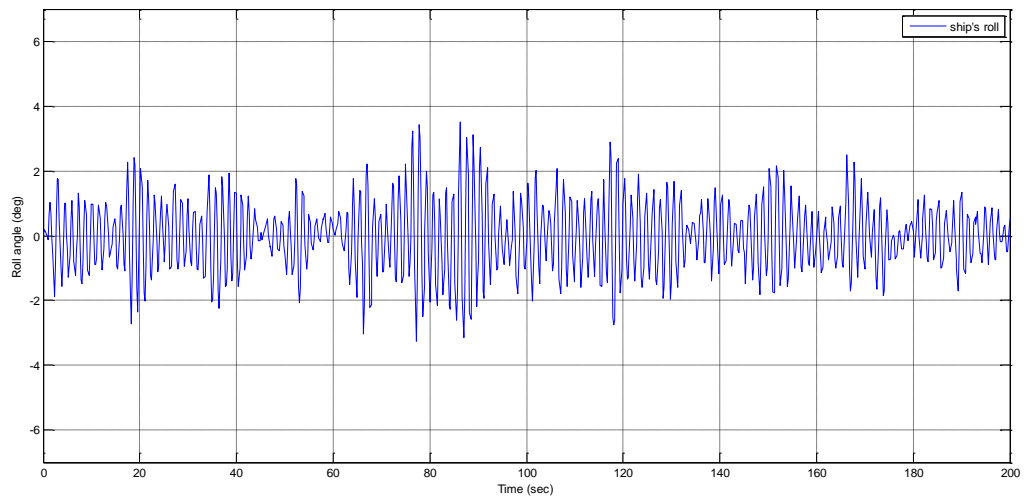


Fig 5.5 Roll angle of ship "A" using NN controller

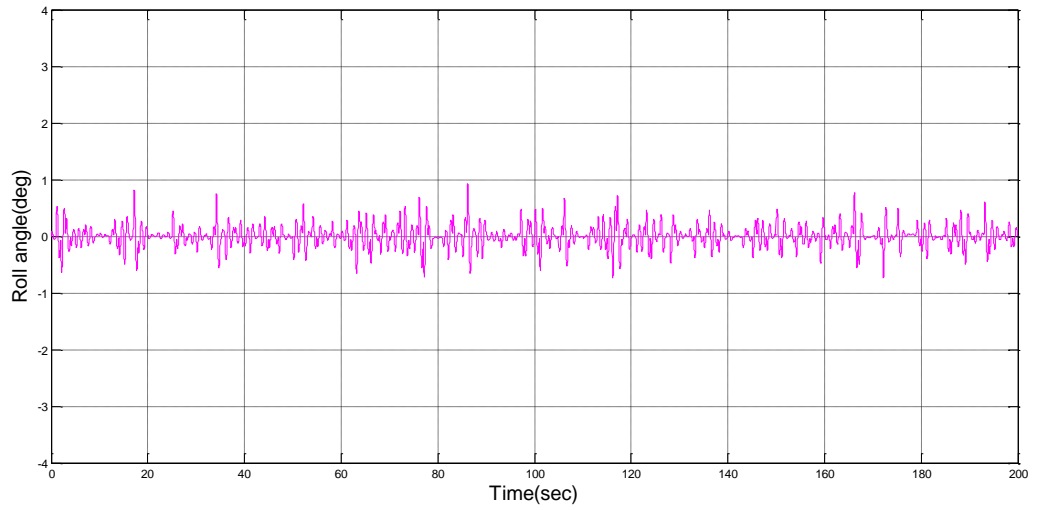


Fig 5.6 Roll angle of ship "B" using PID controller

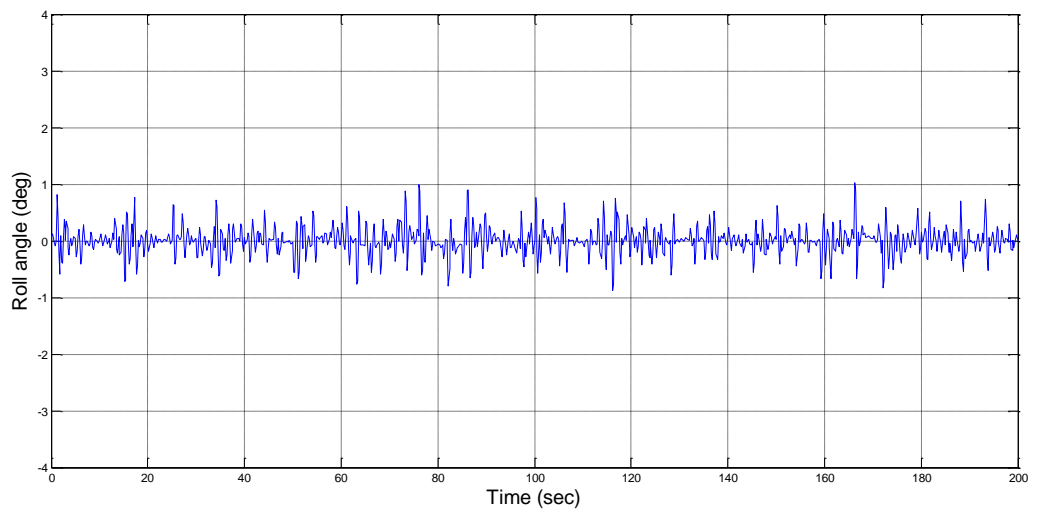


Fig 5.7 Roll angle of ship "B" using NN controller

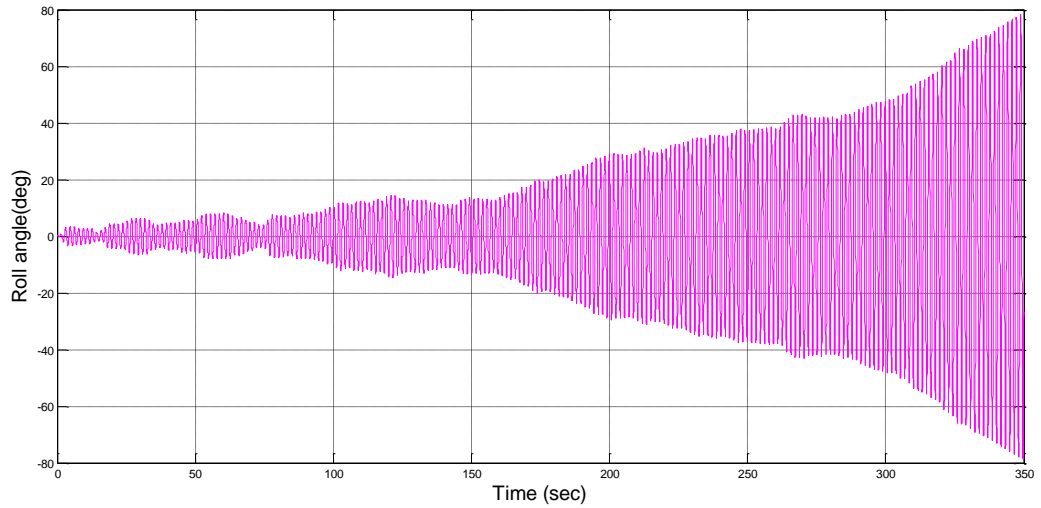


Fig 5.8 Roll angle of ship "C" using PID controller

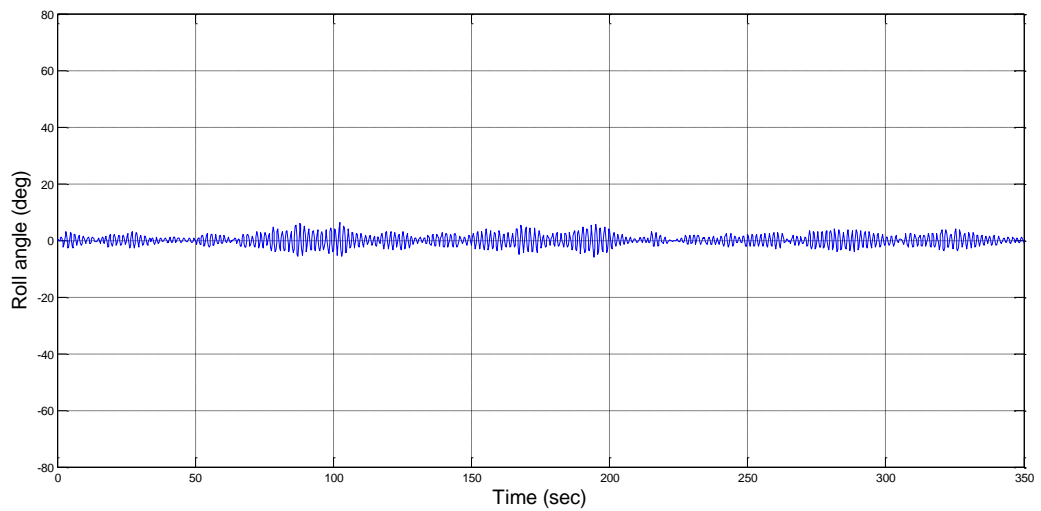


Fig 5.9 Roll angle of ship "C" using NN controller

The **RMS roll angle in all the cases** plotted above have been calculated and compiled in to a table given below:

Table 5.1. Roll angle(RMS) comparison between PID and NN controllers

Ship Condition	PID (deg)	Neural Network (deg)	Change (deg)
A	0.82	1.1	0.28
B	0.19	0.25	0.06
C	8.84	2.11	-6.73

5.4 Reduction of Statistics of Roll (RSR). The RMS values can also be expressed in terms of Reduction of Statistics of Roll (RSR) value. It can be calculated as shown below:

$$RSR = 100\left(1 - \frac{S_s}{S_u}\right) \quad (18)$$

Where,

S_s = RMS value of stabilized roll motion

S_u = RMS value of unstabilized roll motion

By calculating RSR values from the RMS values specified in the above table, we get the below table:

Table 5.2. Roll angle(RSR) comparison between PID and NN controllers

Ship Condition	PID (%)	Neural Network (%)	Change (%)
A	88	84	-4.0
B	97.2	96.3	-0.9
C	-28.5	69.3	97.8

5.5 Neural Network Controller with 2-Inputs. In pursuit to improve the performance of this neural network, a neural network was trained in a similar method as explained before with a change in number of inputs used for training. Here, an additional input in the form of roll rate has also been used to train the neural network along with the error signal. 10 neurons were used in the hidden layer of neural network controller. The block diagram for training the neural network from PID controller and the trained system with NN controller are given below:

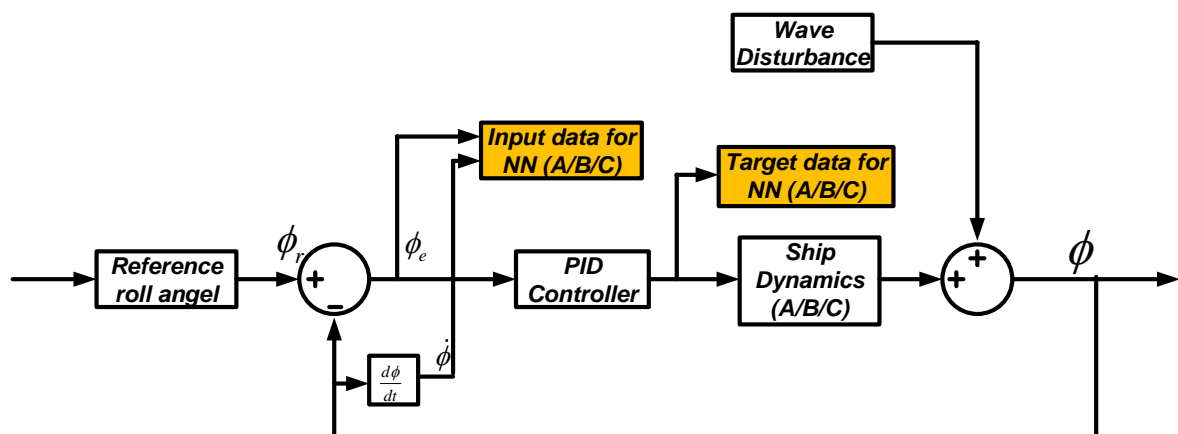


Fig 5.10 Training of NN controller using 2 inputs and 1 target

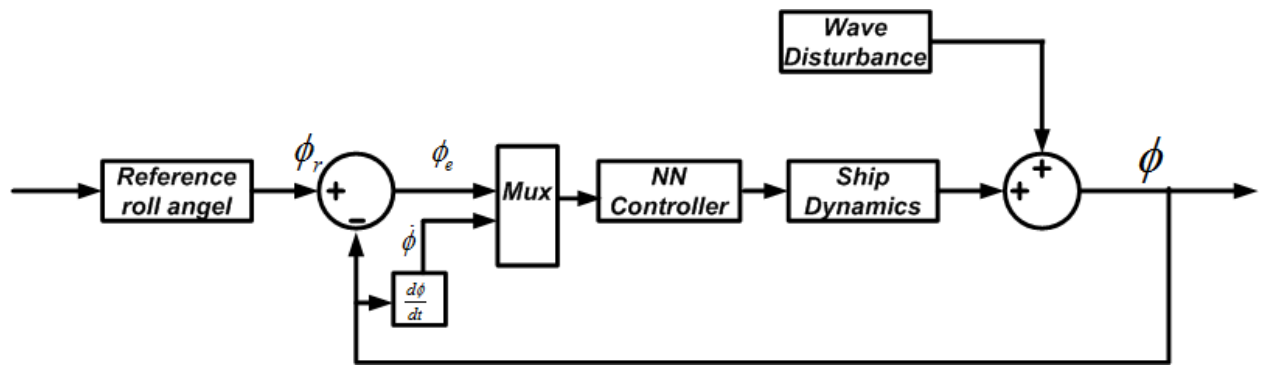


Fig 5.11 Ship's roll control using NN controller with 2 inputs

The ship's roll of the systems A,B and C with NN controller with two inputs is plotted as shown below:

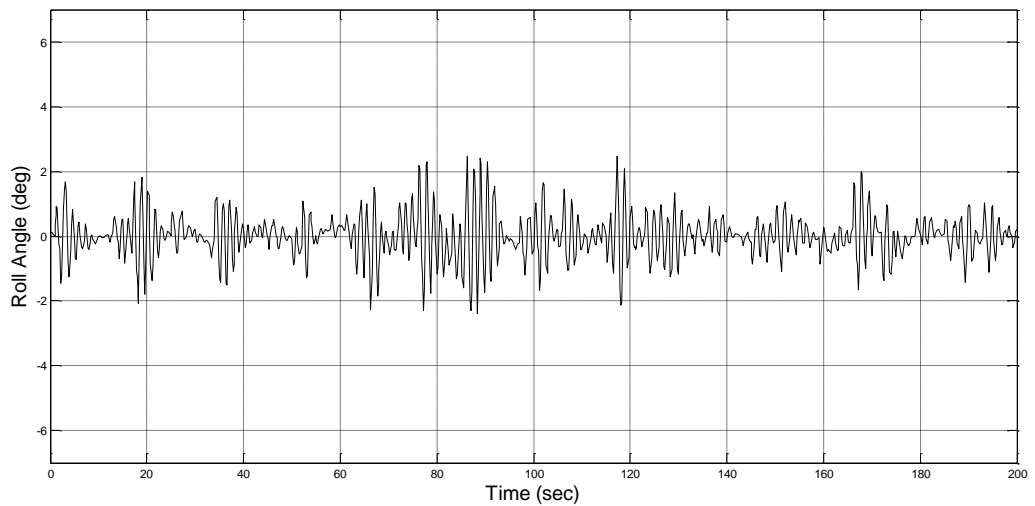


Fig 5.12 Roll angle of ship "A" using 2-input NN controller

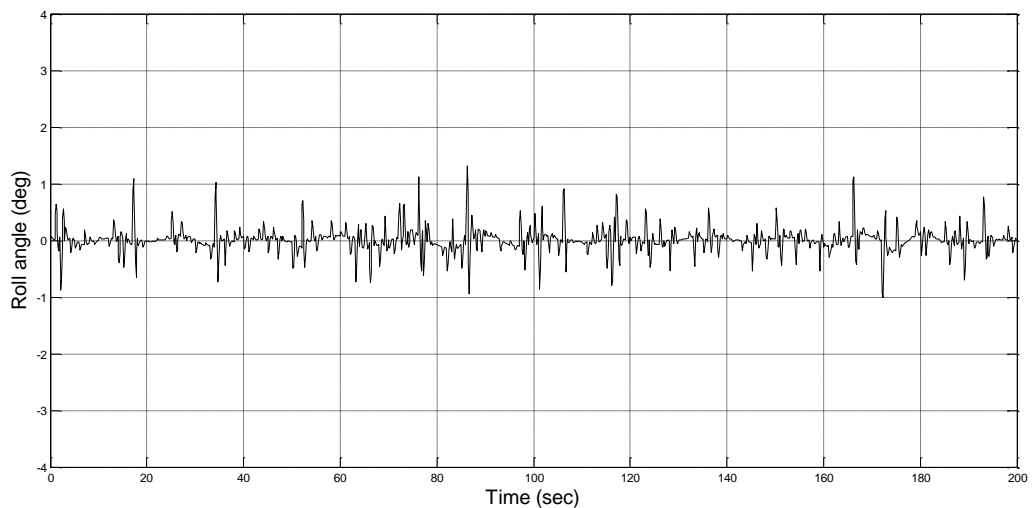


Fig 5.13 Roll angle of ship "B" using 2-input NN controller

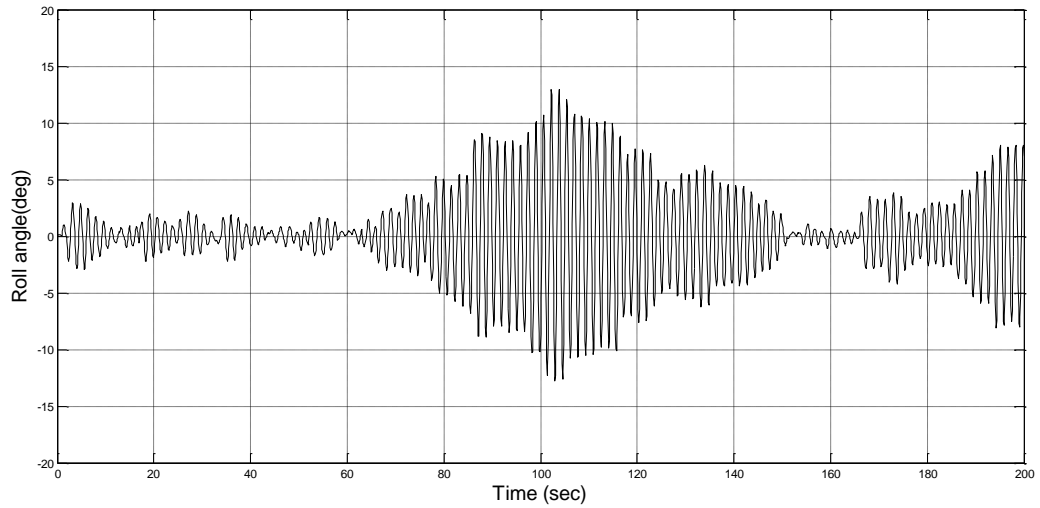


Fig 5.14 Roll angle of ship "C" using 2-input NN controller

5.6 Neural Network Controller with 3-Inputs. After using NN controller with 2 inputs, another neural network was trained in a similar method as explained before with a change in number of inputs used for training. Here, an additional input in the form of roll acceleration along with roll error and roll rate has been used to train the neural network . 10 neurons were used in the hidden layer of neural network controller. The block diagram for training the neural network from PID controller and the trained system with NN controller are given below:

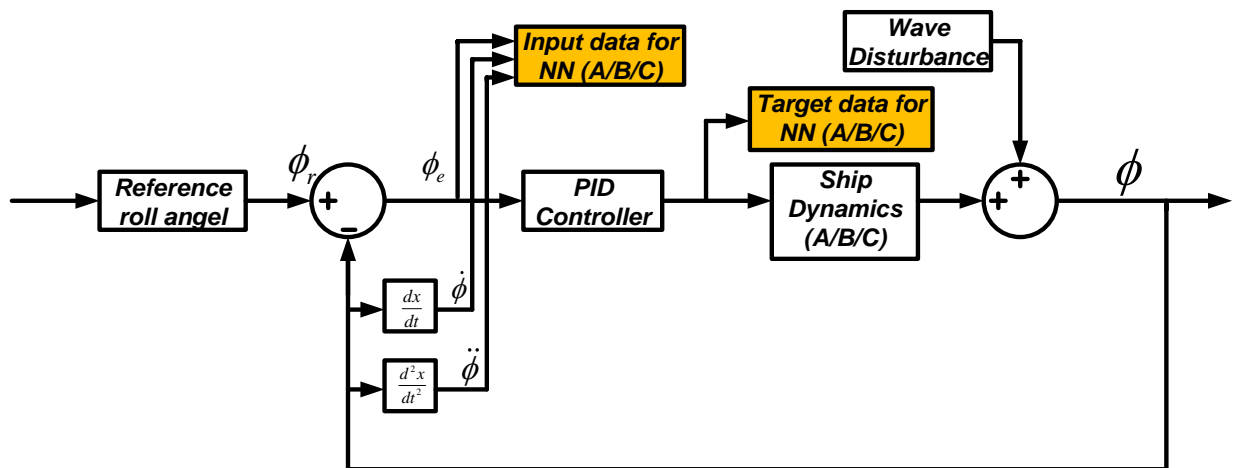


Fig 5.15 Training of NN controller using 2 inputs and 1 target

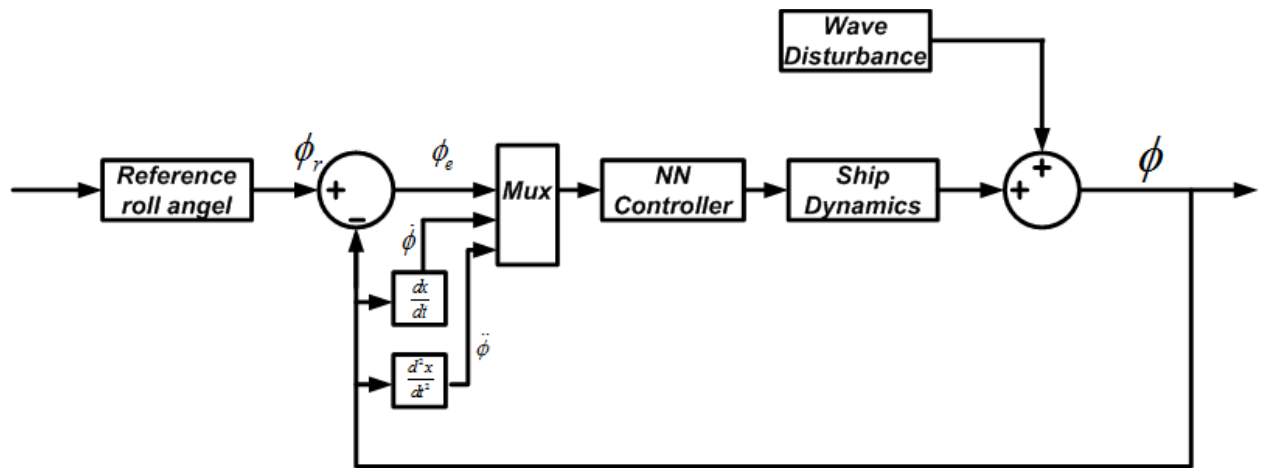


Fig 5.16 Ship's roll control using NN controller with 3 inputs

The ship's roll of the systems A,B and C with NN controller with three inputs is plotted as shown below:

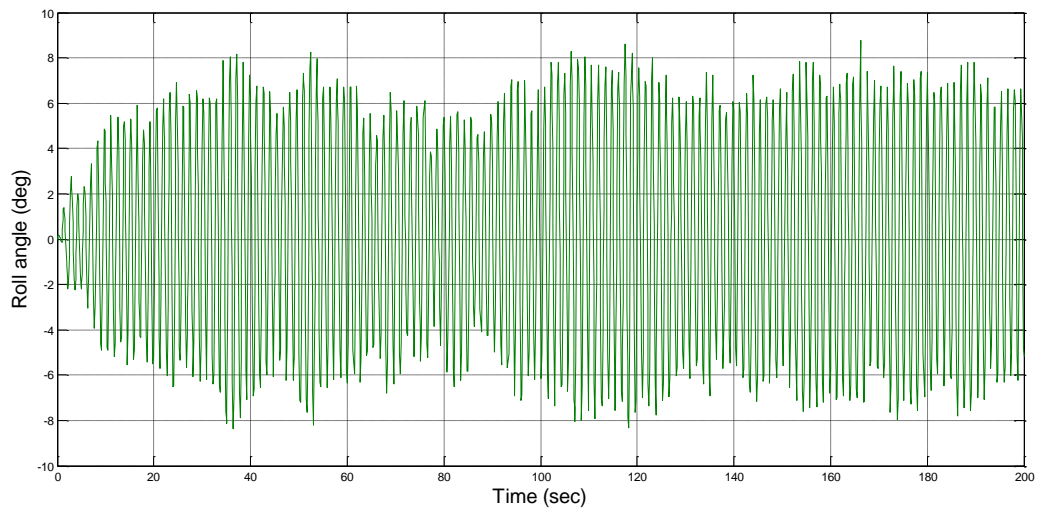


Fig 5.17 Roll angle of ship "A" using 3-input NN controller

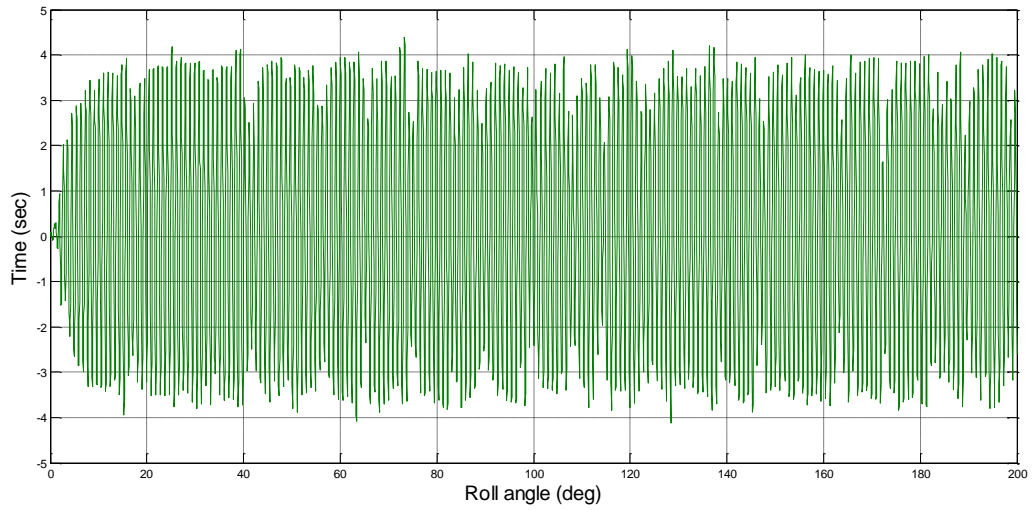


Fig 5.18 Roll angle of ship "B" using 3-input NN controller

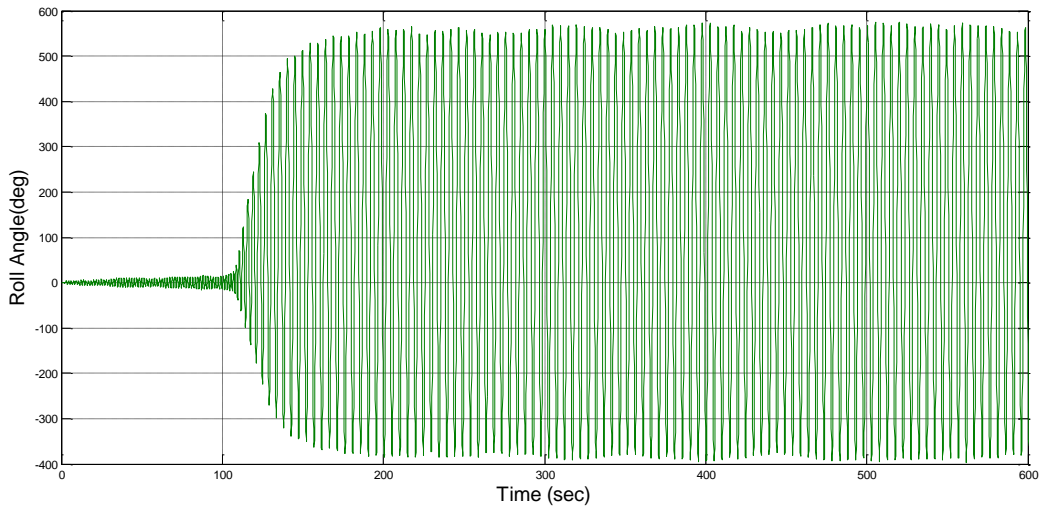


Fig 5.19 Roll angle of ship "C" using 3-input NN controller

The consolidated result of the above mentioned neural networks is specified below:

Table 5.3. Roll angle(RMS) comparison between NN controllers with different number of inputs

Ship Condition	1-Input NN Controller (deg)	2-Input NN Controller (deg)	3-Input NN Controller (deg)
A	1.1	0.7	4.53
B	0.25	0.23	2.59
C	2.11	3.66	343.97

Table 5.4. Roll angle (RSR) comparison between NN controllers with different number of inputs

Ship Condition	1-Input NN Controller(%)	2-Input NN Controller(%)	3-Input NN Controller(%)
A	84	89.8	34.2
B	96.3	96.7	62.4
C	69.3	46.8	-4899.8

Analysing the above data, it is very clear that the best performance is achieved using 2-input NN controller.

5.7 Number of Hidden Neurons. In pursuit to further improve the output/ship's roll, the neural network trained with 2 inputs and 1 target was trained with varying number of hidden neurons ranging from 3 to 100 hidden neurons. Roll angle (RMS and RSR) comparison between NN controllers with different number of hidden neurons is calculated and tabulated in the below tables:

Table 5.5. Roll angle (RMS) comparison between NN controllers with different number of hidden neurons

No of Neurons	A (deg)	B (deg)	C (deg)
3	1.4108	0.2586	3.8162
5	0.8507	0.2446	3.6365
10	0.703	0.2286	3.6576
20	0.6961	0.2254	3.4224
24	0.723	0.2147	3.5261
25	0.648	0.2221	3.5472
26	0.6777	0.2245	3.7055
30	0.7233	0.2133	3.7
50	0.6593	0.2282	3.6981
100	0.7001	0.2469	3.7501

Table 5.6. Roll angle (RSR) comparison between NN controllers with different number of hidden neurons

No of Neurons	A	B	C
3	79.5 %	96.2 %	44.5 %
5	87.6 %	96.4 %	47.1 %
10	89.8 %	96.7 %	46.8 %
20	89.9 %	96.7 %	50.3 %
24	89.5 %	96.9 %	48.7 %
25	90.6 %	96.8 %	48.4 %
26	90.1 %	96.7 %	46.1 %
30	89.5 %	96.9 %	46.2 %
50	90.4 %	96.7 %	46.2 %
100	89.8 %	96.4 %	45.5 %

The above data is depicted below in the form of a graph:

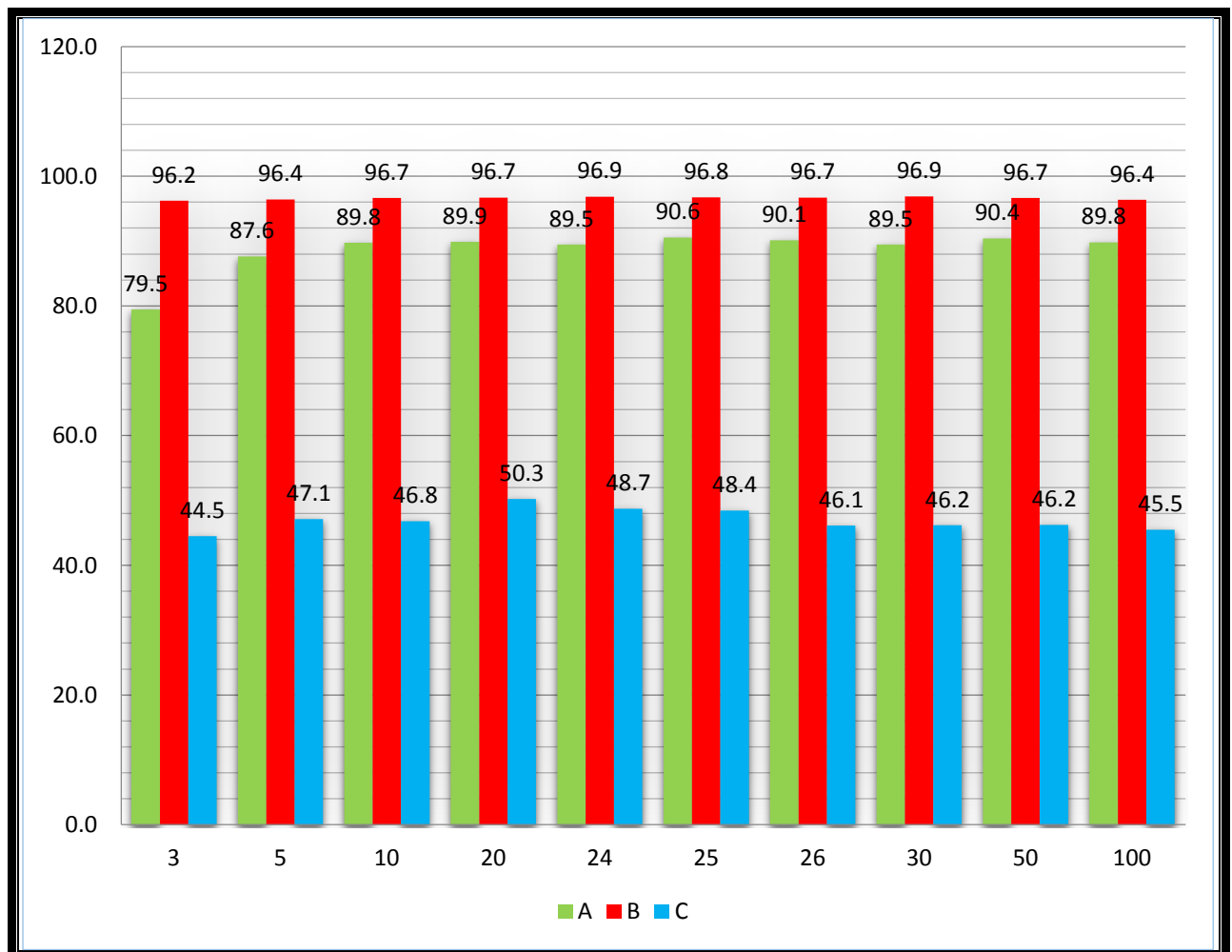


Fig 5.20 RSR roll angle with different number of hidden neurons in NN controller

The ship's roll angle or the plant's output by using NN controller with 25 hidden neurons in all the three cases(A/B/C) are plotted below:

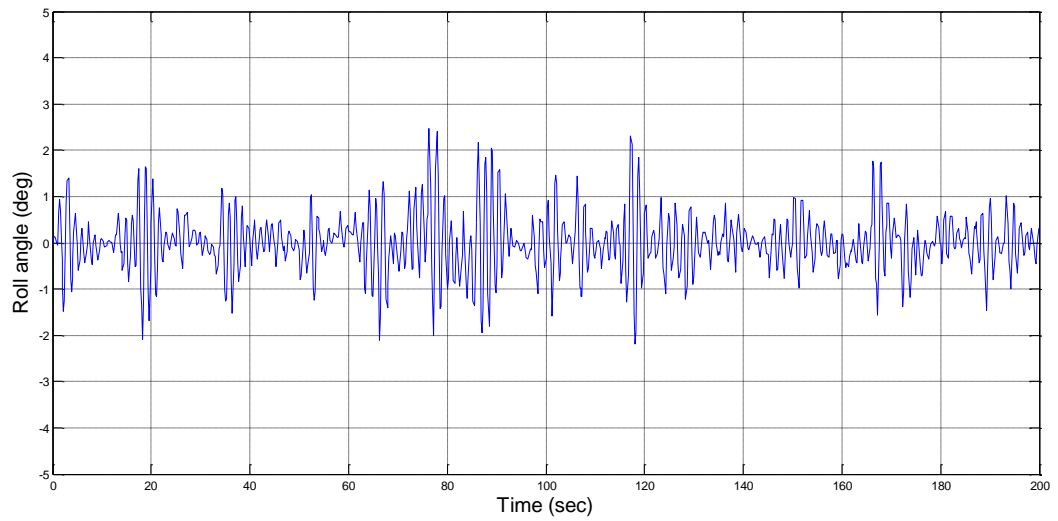


Fig 5.21 Roll angle of ship "A" using 2-input NN controller with 25 hidden neurons

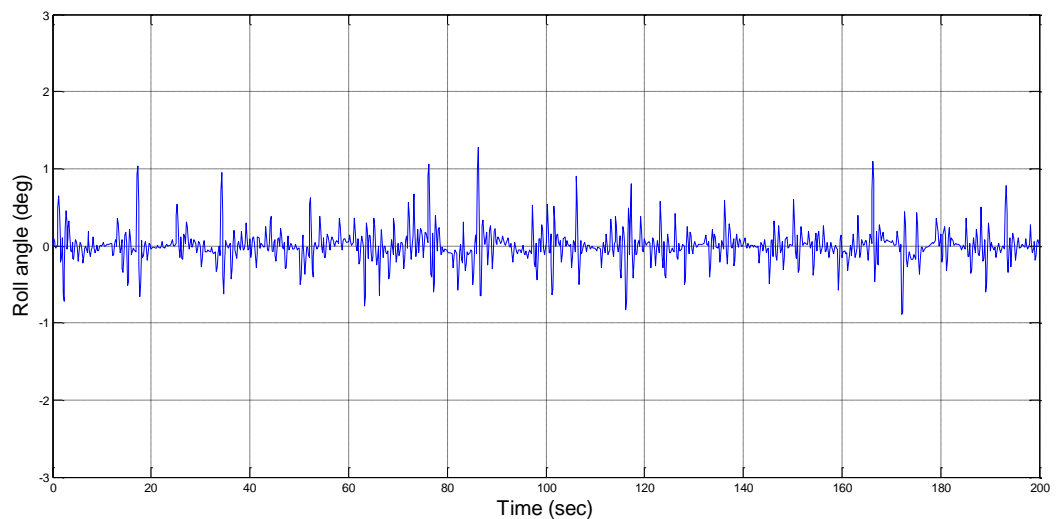


Fig 5.22 Roll angle of ship "B" using 2-input NN controller with 25 hidden neurons

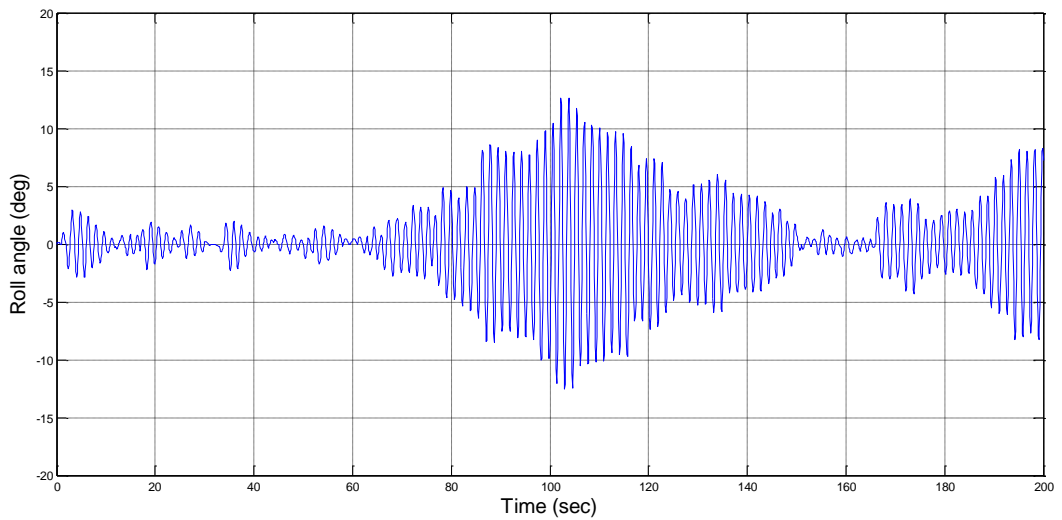


Fig 5.23 Roll angle of ship "C" using 2-input NN controller with 25 hidden neurons

The ship's response (roll angle - RMS and RSR) is compared between the initially designed PID controller and the final neural network with 25 neurons is compared in the following tables:

Table 5.7. Roll angle(RMS) comparison between PID and NN controller with 25 hidden neurons

Ship Condition	PID(Deg)	Neural Network (Deg)	Change (Deg)	Remarks
A	0.823	0.648	-0.17	Improved
B	0.193	0.221	0.02	Almost Same
C	8.84(sink)	3.547	Ship saved	Ship saved from sinking

Table 5.8. Roll angle(RSR) comparison between PID and NN controller with 25 hidden neurons

Ship Condition	PID (%)	Neural Network (%)	Change (%)	Remarks
A	88.04	90.58	2.5 %	Improved
B	97.19	96.77	-0.4 %	Almost Same
C	sink	48.44	Ship saved	Ship saved from sinking

It is very evident from the above table and graphs that the ship's roll response has:

- (a) improved in ship 'A'.
- (b) almost remained the same in ship 'B'.
- (c) improved a lot and **saved the ship from sinking** in ship 'C'.

Chapter 6

Saturation Limits Of Stabilizers Fins

6.1 Introduction

The active fin stabilisers which are used to control the ship's roll are a set of 2 fins which rotate in opposite directions at any given time to create a desired transverse angular moment to the ship. The fins are so designed that there is a physical limit in their rotation angle. All equipments related to the stabilisers are designed accordingly.

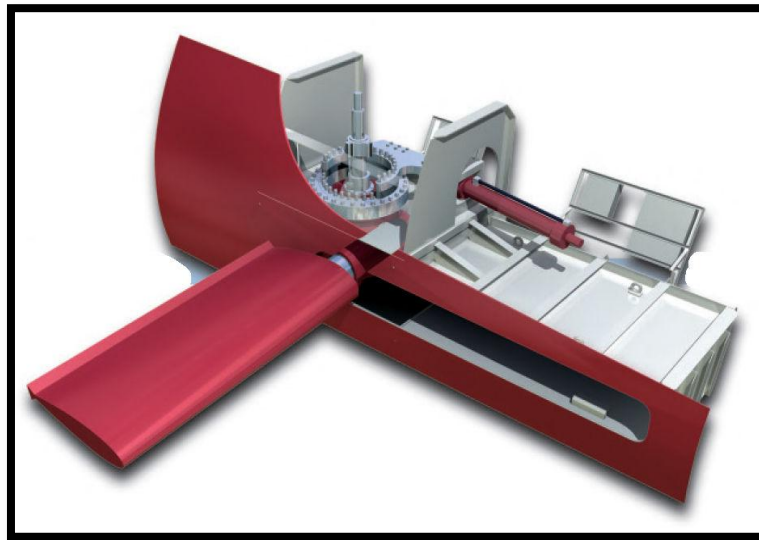


Fig 6.1 Cut section of a stabilizer and its auxiliary machinery[31]

Generally, the fins can rotate from -30 to +30 degrees. This a physical constraint on the mechanical equipment and value more than the designed limits are not possible.

6.2 Common Mistake by Researchers

In many technical papers and simulations used for controlling the ship's roll, it is common to see that the saturation value or the physical limitation on the fin angle is not considered by the researchers. It is also pertinent to mention that 360 degree angle of the fin is equal to '0' degree and is not going to provide any control action for the ship's roll. The below figure[10] is an example of a simulation which considered a fin angle of 260 degrees which is not practically viable.

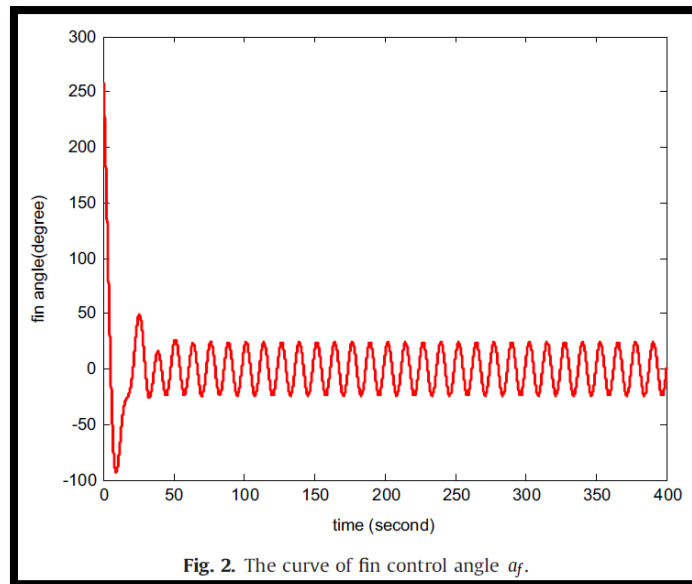


Fig 6.2 Figure showing impractical fin angles considered by a researcher[10]

6.3 Saturation Limits

To remove this gap existing between the practical stabilisers and simulations worked upon in the previous chapters, new set of PID controllers were designed with saturation values.

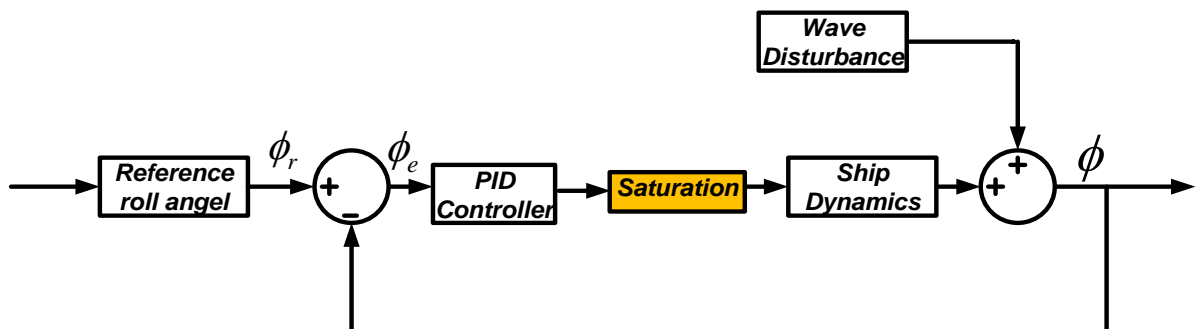
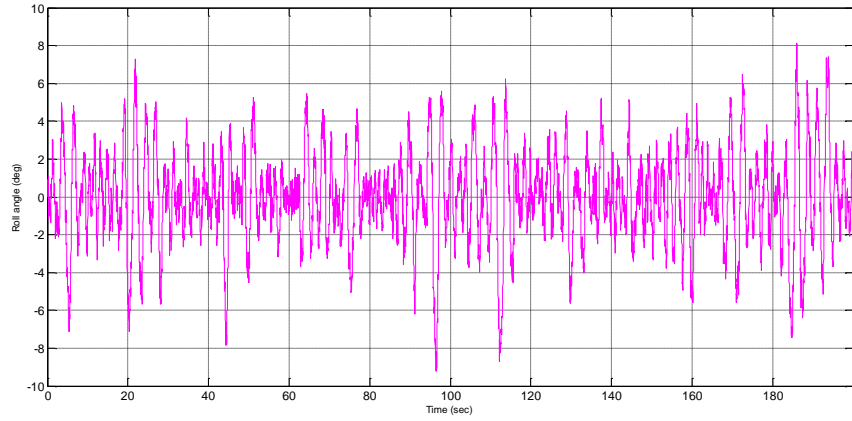
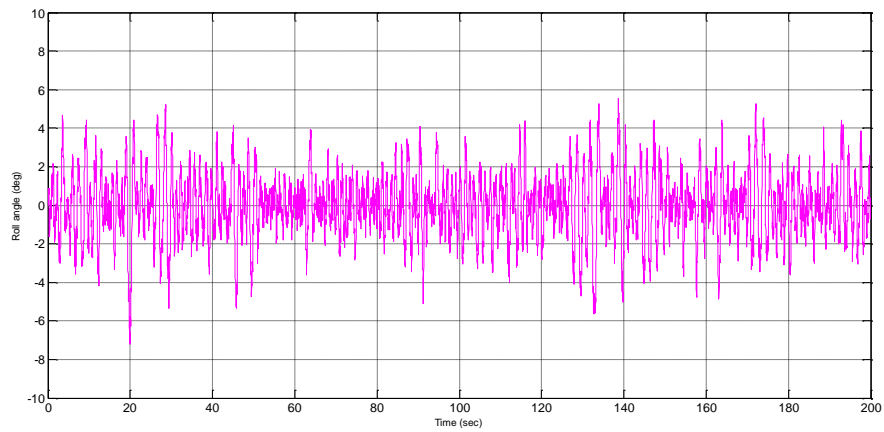


Fig 6.3 Block Diagram of the system controlled by PID controller with saturation

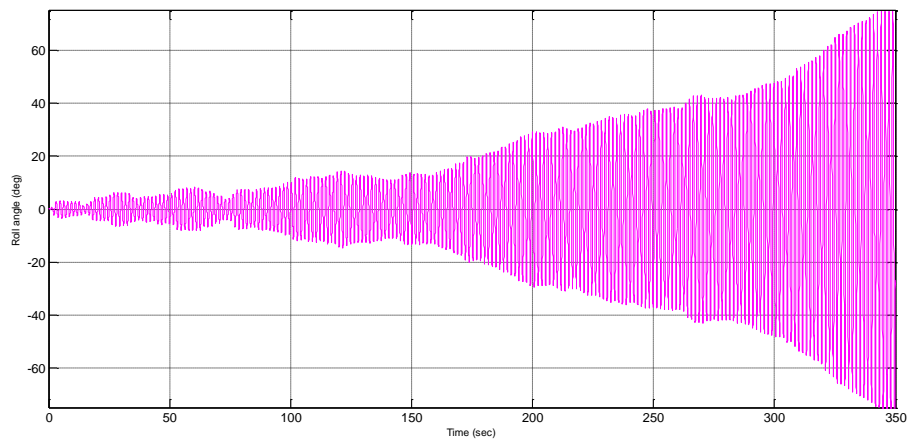
The upper limit for the control signal was chosen to be 30 units and the lower limit to be -30 units. After choosing the saturation limits, PID controller was redesigned for the initially considered ship and the output of the ship(roll angle) is given below in all the 3 cases of the ship(A,B and C):



(Ship "A")



(Ship "B")



(Ship "C")

Fig 6.4 Roll angles of ship A,B & C using PID controller with saturation limits

To improve this roll stabilization, 3 separate PID controllers were designed for the 3 cases of the ship considered before(A,B and C) in the same manner as explained in

the previous chapters. Data was extracted from these PID controllers to design neural network based controller with 2 inputs(error signal and derivative of feedback signal) and 28 hidden neurons.

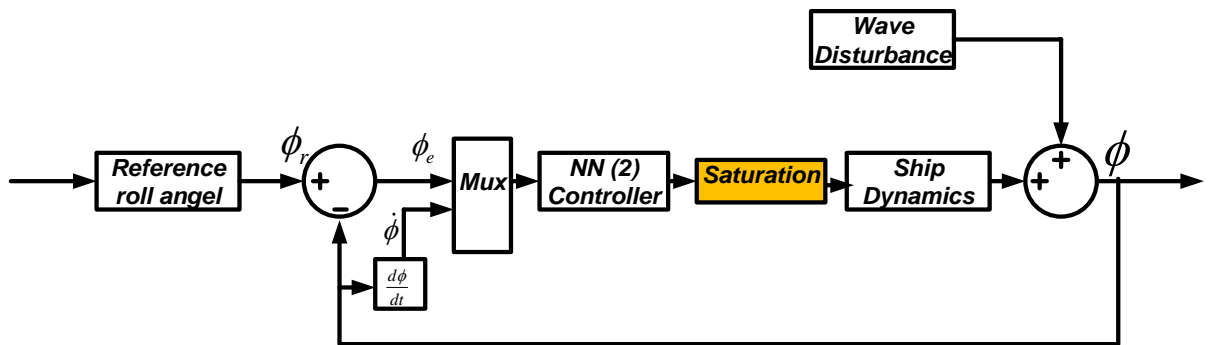


Fig 6.5 Block Diagram of the Ship's roll control by NN controller with saturation

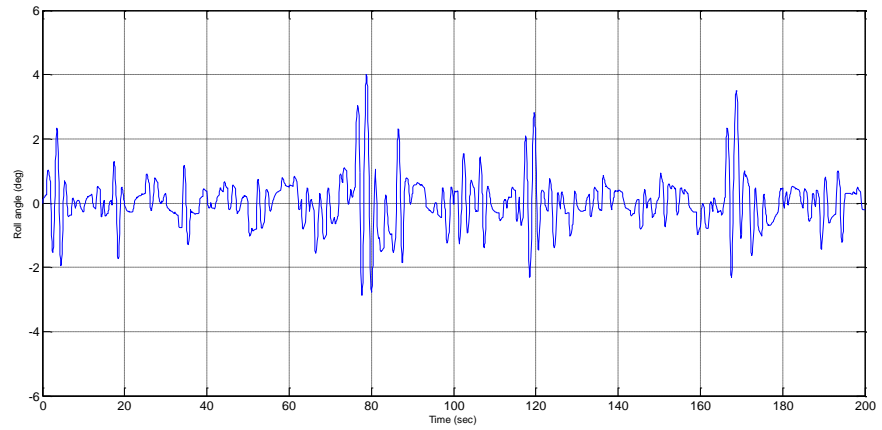
The ship's roll using PID control and NN controller is summarized in the below table:

Table 6.1. Ship's roll angle using PID and NN controllers with saturation

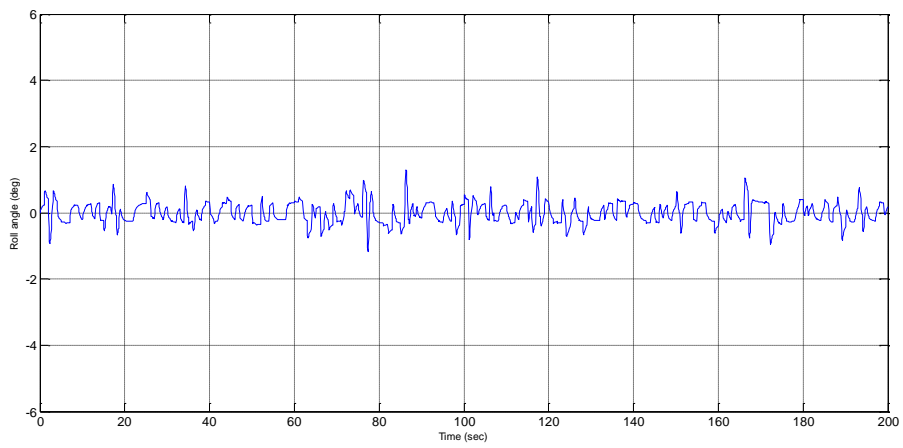
Ship Condition	PID (Deg)	Neural Network (Deg)
A	2.4534	1.2264
B	1.7111	0.3594
C	8.844	3.9782

By observing table no. 6.1, it is very evident that after considering saturation limits of the stabilizer fin rotation angles, the NN controller performed better than the PID controller as observed even without saturation condition. However, as the fin angle was restricted to 30 degs on both sides, the control action is lesser than the expected values derived from simulations in the previous chapters.

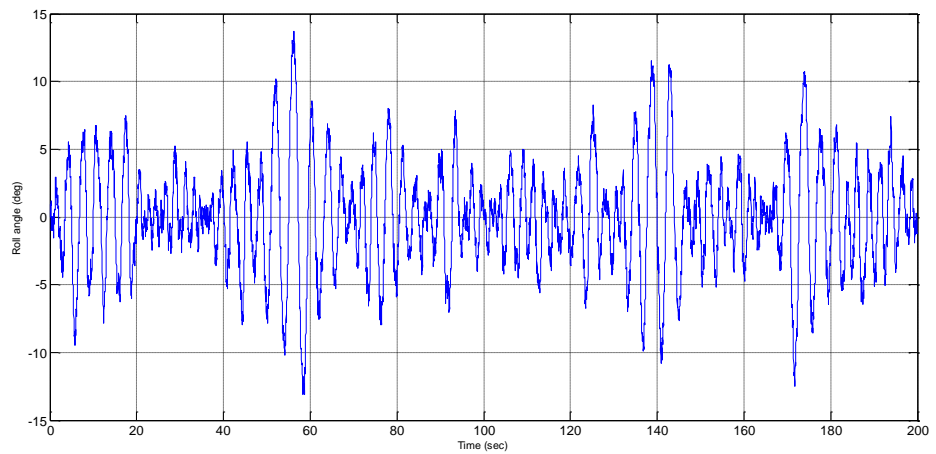
The ship's roll in all the 3 conditions after using the latest designed neural network controller is at Fig 6.6:



(Ship "A")



(Ship "B")



(Ship "C")

Fig 6.6 Roll angle of ship A,B&C using NN controller with saturation limits

Chapter 7

Fuzzy Logic Controller

7.1 Introduction

A fuzzy control system is a control system based on fuzzy logic, mathematical system that analyzes analog input values in terms of logical variables that take on continuous values between 0 and 1, in contrast to classical or digital logic, which operates on discrete values of either 1 or 0 (true or false, respectively)[32, 33]

The input variables in a fuzzy control system are in general mapped by sets of membership functions known as "fuzzy sets". The process of converting a crisp input value to a fuzzy value is called "fuzzification". In practice, the controller accepts the inputs and maps them into their membership functions and truth values. These mappings are then fed into the rules. If the rule specifies an AND relationship between the mappings of the two input variables, the minimum of the two is used as the combined truth value; if an OR is specified, the maximum is used. The appropriate output state is selected and assigned a membership value at the truth level of the premise. The truth values are then defuzzified.[33]

After creating PID and Neural network controller for the ship's roll stabilization, possibility of creating a fuzzy logic controller was envisaged. The main obstacle in the process was to understand the ship's dynamic behavior and accordingly, create the rules for the fuzzy logic controller.

7.2 Shape selection for Membership Functions

Initially a fuzzy logic controller with one input and one output was created as a replacement to the initially designed PID controller. Five equal sized and spaced Gaussian membership functions(MFs) were created for both input and output fuzzy set of the fuzzy logic controller(FLC). Here, controller's actual input-output relation rules of the practical ships roll were not available for designing the FLC. So, the input and output data of the PID controller (error signal and control signal) which are separately tuned in each of the three cases(A,B,C) were used in designing FLC. This PID data had more than 60,000 samples. The minimum and maximum values of the PID input-output data was used to decide range of the input and output fuzzy sets of the FLC. The 5 MFs of input and output fuzzy sets are named as mf1, mf2, mf3, mf4 and mf5 in sequence.

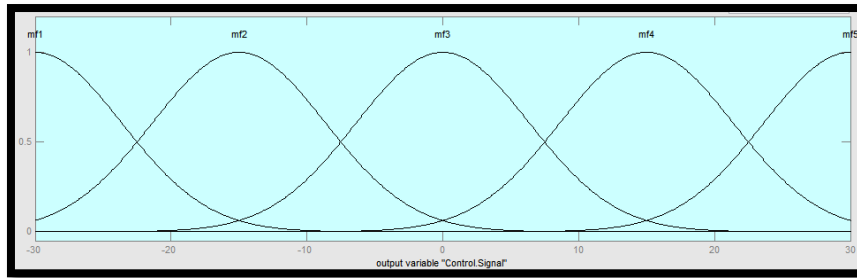


Fig. 7.1 Output fuzzy set with Gaussian membership functions

By analysing the PID data base created earlier, 5 ruled were made and applied to the FLC. Once the FLC was designed, it replaced the PID controller in the ship's roll control system and the performance was checked for all the 3 cases of the ship (A,B and C).

Thereafter the input and output Gaussian mfs were replaced with various shaped MFs and compared for performance. The RMS values of the ship's roll is appended below:

Table 7.1. Roll angle(RMS) comparison between various type of fuzzy sets

Membership function's Shape	Ship Condition		
	A	B	C
Gaussian	2.8855	2.2867	3.6030
Triangle	3.0818	2.2585	4.6818
Trapezium	3.1317	2.2235	4.8281
Gaussian bell	2.9291	2.2574	3.8988
Gaussian 2	2.9312	2.2680	3.5842

By analyzing the above results, it was understood that Gaussian fuzzy sets(input and output) gave better results than other type of fuzzy sets. The control surface used is shown below:

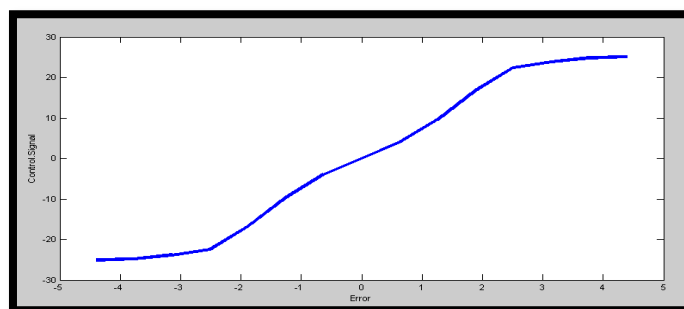


Fig 7.2 Control surface of 1-input FLC with 5 rules

7.3 Fuzzy Logic Controller with 2-Inputs

In pursuit to improve the performance of the designed FLC, a FLC was designed in a similar method as explained before with a change in number of inputs. Here, a second input in the form of roll rate along with the error signal has also been used as an input to the FLC.

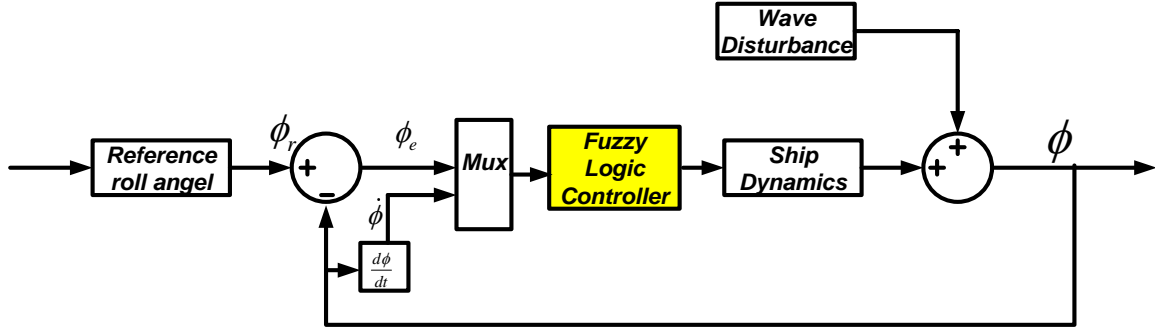


Fig 7.3 Ship's roll control using FLC with 2 inputs

As the rules for FLC were not known, the same were derived by analysing the PID input-output data.

7.3.1 Methodology for Deriving Fuzzy Rules

From the PID input-output data, 3 values were used:

Table 7.2. PID signals used for FLC design

<u>Sl No</u>	<u>Signal from PID controlled plant</u>	<u>Nomenclature of PID signals</u>	<u>Corresponding FLC signal</u>
(a)	Error signal	Input-1	Input-1
(b)	Derivative of roll angle/feedback	Input-2	Input-2
(c)	Control signal	Output	Output

- The range of the input-1 of the FLC was initially decided by the maximum and minimum value of the input-1 data of PID input-output data.
- The range was divided in to five equal parts. Here, each range corresponds to one MF of input-1 fuzzy set(mf1,mf2,mf3,mf4 and mf5) of FLC.
- Input-1 of each sample in the PID database was assigned a MF.
- The same procedure was used on every sample in the PID database to assign a MF for Input-2 and output also.
- Since there are 3 variables(input-1, input-2 and output) and each variable has 5 MFs, there are a total of (5x5x5 =) 125 possible sets of combinations into which each PID sample will be segregated into based on its input and output MFs.
-

Frequency of each set was calculated and tabulated below:

Table 7.3. Grouping of PID database for FLC rules creation

SI No	Membership Function of			Freq	Weigh-tage
	Ip-1	Ip-2	Op		
1	mf1	mf1	mf1	2	0.00008
2	mf1	mf1	mf2	0	0
3	mf1	mf1	mf3	0	0
4	mf1	mf1	mf4	0	0
5	mf1	mf1	mf5	0	0
6	mf1	mf2	mf1	56	0.00224
7	mf1	mf2	mf2	0	0
8	mf1	mf2	mf3	2	0.00008
9	mf1	mf2	mf4	1	0.00004
10	mf1	mf2	mf5	0	0
11	mf1	mf3	mf1	350	0.014
12	mf1	mf3	mf2	17	0.00068
13	mf1	mf3	mf3	0	0
14	mf1	mf3	mf4	0	0
15	mf1	mf3	mf5	0	0
16	mf1	mf4	mf1	62	0.00248
17	mf1	mf4	mf2	0	0
18	mf1	mf4	mf3	0	0
19	mf1	mf4	mf4	0	0
20	mf1	mf4	mf5	0	0
21	mf1	mf5	mf1	0	0
22	mf1	mf5	mf2	0	0
23	mf1	mf5	mf3	0	0
24	mf1	mf5	mf4	0	0
25	mf1	mf5	mf5	0	0
26	mf2	mf1	mf1	56	0.00224
27	mf2	mf1	mf2	0	0
28	mf2	mf1	mf3	0	0
29	mf2	mf1	mf4	0	0
30	mf2	mf1	mf5	0	0
31	mf2	mf2	mf1	383	0.01532
32	mf2	mf2	mf2	9	0.00036
33	mf2	mf2	mf3	3	0.00012
34	mf2	mf2	mf4	13	0.00052
35	mf2	mf2	mf5	50	0.002
36	mf2	mf3	mf1	1138	0.04552
37	mf2	mf3	mf2	367	0.01468
38	mf2	mf3	mf3	433	0.01732

SI No	Membership Function of			Freq	Weigh-tage
	Ip-1	Ip-2	Op		
39	mf2	mf3	mf4	0	0
40	mf2	mf3	mf5	3	0.00012
41	mf2	mf4	mf1	540	0.0216
42	mf2	mf4	mf2	1	0.00004
43	mf2	mf4	mf3	0	0
44	mf2	mf4	mf4	0	0
45	mf2	mf4	mf5	0	0
46	mf2	mf5	mf1	16	0.00064
47	mf2	mf5	mf2	0	0
48	mf2	mf5	mf3	0	0
49	mf2	mf5	mf4	0	0
50	mf2	mf5	mf5	0	0
51	mf3	mf1	mf1	18	0.00072
52	mf3	mf1	mf2	25	0.001
53	mf3	mf1	mf3	31	0.00124
54	mf3	mf1	mf4	39	0.00156
55	mf3	mf1	mf5	33	0.00132
56	mf3	mf2	mf1	171	0.00684
57	mf3	mf2	mf2	303	0.01212
58	mf3	mf2	mf3	376	0.01504
59	mf3	mf2	mf4	440	0.0176
60	mf3	mf2	mf5	578	0.02312
61	mf3	mf3	mf1	3770	0.1508
62	mf3	mf3	mf2	7803	0.31212
63	mf3	mf3	mf3	25686	1.02744
64	mf3	mf3	mf4	7433	0.29732
65	mf3	mf3	mf5	3847	0.15388
66	mf3	mf4	mf1	638	0.02552
67	mf3	mf4	mf2	464	0.01856
68	mf3	mf4	mf3	475	0.019
69	mf3	mf4	mf4	348	0.01392
70	mf3	mf4	mf5	141	0.00564
71	mf3	mf5	mf1	42	0.00168
72	mf3	mf5	mf2	22	0.00088
73	mf3	mf5	mf3	20	0.0008
74	mf3	mf5	mf4	10	0.0004
75	mf3	mf5	mf5	6	0.00024
76	mf4	mf1	mf1	0	0
77	mf4	mf1	mf2	0	0

<u>Sl No</u>	<u>Membership Function of</u>			<u>Freq</u>	<u>Weigh-tage</u>
78	mf4	mf1	mf3	0	0
79	mf4	mf1	mf4	0	0
80	mf4	mf1	mf5	19	0.00076
81	mf4	mf2	mf1	0	0
82	mf4	mf2	mf2	0	0
83	mf4	mf2	mf3	0	0
84	mf4	mf2	mf4	7	0.00028
85	mf4	mf2	mf5	475	0.019
86	mf4	mf3	mf1	0	0
87	mf4	mf3	mf2	40	0.0016
88	mf4	mf3	mf3	440	0.0176
89	mf4	mf3	mf4	616	0.02464
90	mf4	mf3	mf5	1412	0.05648
91	mf4	mf4	mf1	6	0.00024
92	mf4	mf4	mf2	16	0.00064
93	mf4	mf4	mf3	14	0.00056
94	mf4	mf4	mf4	14	0.00056
95	mf4	mf4	mf5	446	0.01784
96	mf4	mf5	mf1	0	0
97	mf4	mf5	mf2	0	0
98	mf4	mf5	mf3	0	0
99	mf4	mf5	mf4	4	0.00016
100	mf4	mf5	mf5	19	0.00076
101	mf5	mf1	mf1	0	0

<u>Sl No</u>	<u>Membership Function of</u>			<u>Freq</u>	<u>Weigh-tage</u>
102	mf5	mf1	mf2	0	0
103	mf5	mf1	mf3	0	0
104	mf5	mf1	mf4	0	0
105	mf5	mf1	mf5	0	0
106	mf5	mf2	mf1	0	0
107	mf5	mf2	mf2	0	0
108	mf5	mf2	mf3	0	0
109	mf5	mf2	mf4	0	0
110	mf5	mf2	mf5	35	0.0014
111	mf5	mf3	mf1	0	0
112	mf5	mf3	mf2	0	0
113	mf5	mf3	mf3	0	0
114	mf5	mf3	mf4	0	0
115	mf5	mf3	mf5	187	0.00748
116	mf5	mf4	mf1	0	0
117	mf5	mf4	mf2	0	0
118	mf5	mf4	mf3	0	0
119	mf5	mf4	mf4	0	0
120	mf5	mf4	mf5	32	0.00128
121	mf5	mf5	mf1	0	0
122	mf5	mf5	mf2	0	0
123	mf5	mf5	mf3	0	0
124	mf5	mf5	mf4	0	0
125	mf5	mf5	mf5	0	0

In the table 7.3, frequency represents the number of samples in the PID database which match with the set of particular MF combination. Weightage is a number proportional to the frequency specified. This weightage is applied to the particular rule. So, for example Sl. No 120 in table 7.3 specifies a rule as mentioned below:

"If (Error is mf5) AND (Roll rate is mf4), then (Control Signal is mf5)". The weightage of this rule 0.00128.

Out of the 125 combinational sets specified in the table, there are 62 rules with non-zero weightage. These rules combine to give the control surface given at Fig.7.4:

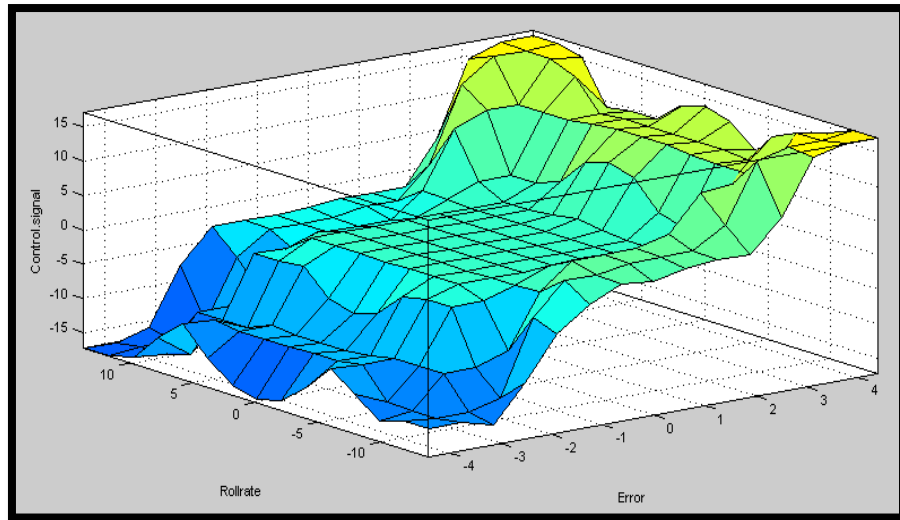


Fig 7.4 Control surface of FLC with equal sized Gaussian MFs and 125 rules

FLC designed using the above control surface for the rules, was tested for its performance and the ship's roll angles are plotted as below:

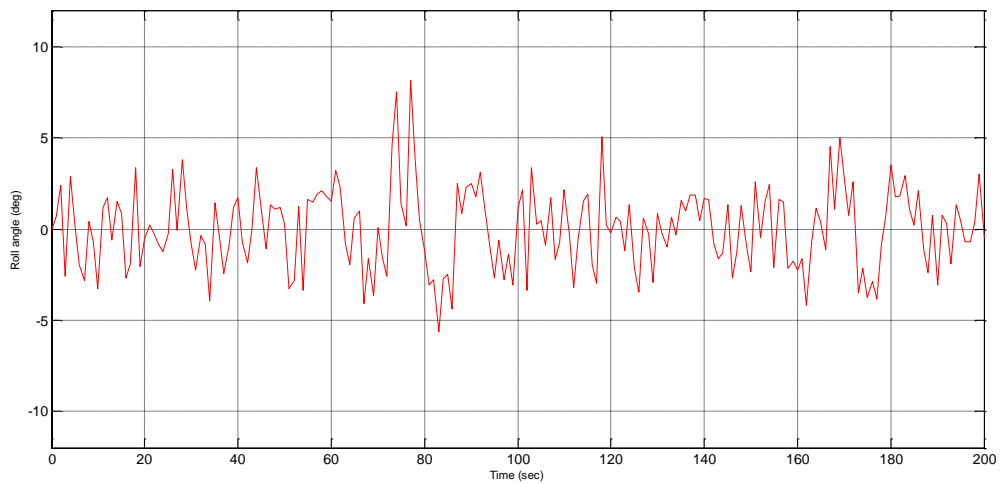


Fig 7.5 Ship's response (A) using FLC with saturation limits and equal sized Gaussian MFs

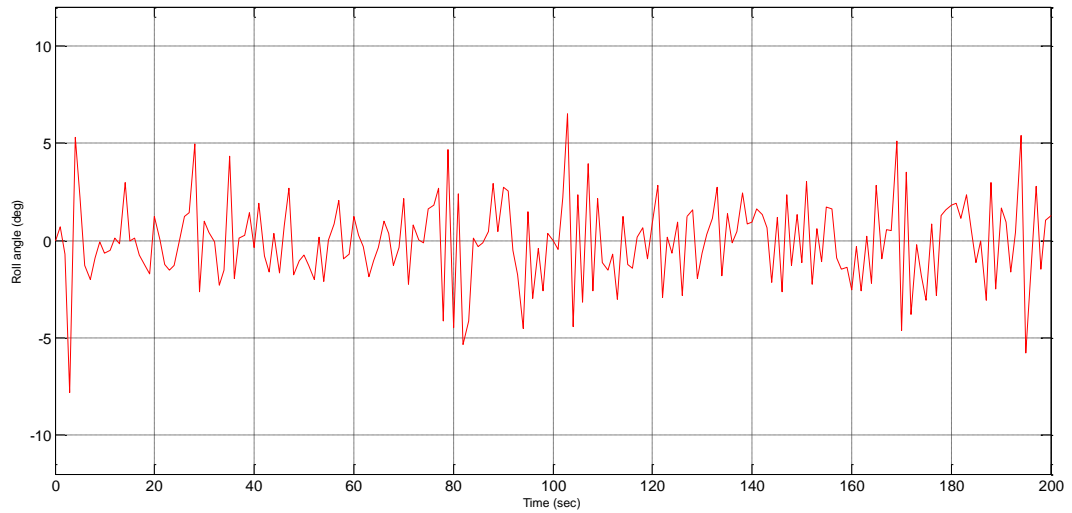


Fig 7.6 Ship's response (B) using FLC with saturation limits and equal sized Gaussian MFs

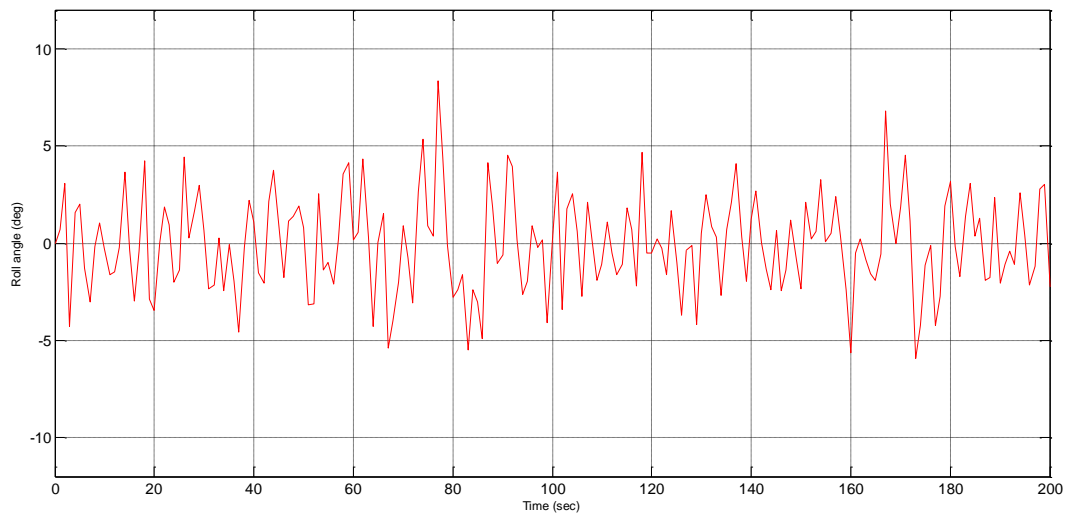


Fig 7.7 Ship's response (C) using FLC with saturation limits and equal sized Gaussian MFs

7.3.2 FLC with 2-Inputs and 25 Rules. From the above table, separate FLC was designed with 25 rules. Here each combination of error and roll rate will be given a MF pertaining to the control signal with maximum samples(freq) from the PID database. The rule table is calculated as tabulated below:

Table 7.4. Fuzzy rules(25) of FLC with equal sized Gaussian MFs

Control Signal		Roll Rate				
		mf1	mf2	mf3	mf4	mf5
Error	mf1	mf1	mf1	mf1	mf1	mf1
	mf2	mf1	mf1	mf1	mf1	mf1
	mf3	mf4	mf5	mf3	mf1	mf1
	mf4	mf5	mf5	mf5	mf5	mf5
	mf5	mf5	mf5	mf5	mf5	mf5

The control surface is shown below:

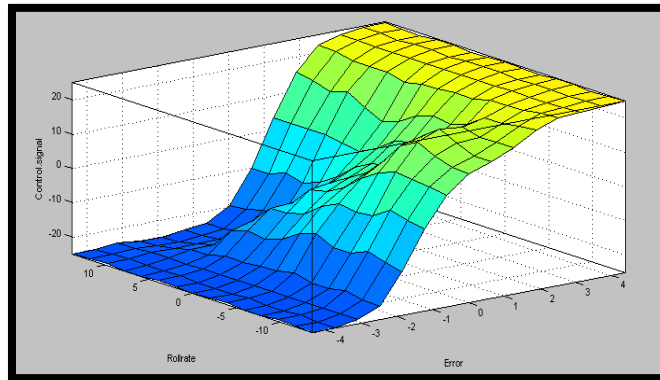


Fig 7.8 Control surface of FLC with equal sized Gaussian MFs and 25 rules

The RMS value of ship's roll (A,B&C) was calculated separately using each of the above mentioned FLC which has 5 rules or 25 rules or 125 rules and tabulated below:

Table 7.5. Ship's roll angle (RMS) using various FLCs with equal sized Gaussian MFs

Ship's Condition	No of rules in the FLC		
	5	25	125
A	4.2112	2.7461	2.5971
B	11.5855	8.8373	2.1237
C	6.6264	2.3550	3.0687

The above table clearly shows that the FLC designed with 125 rules performed much better to the FLC designed with 25 rules or 5 rules.

7.4 FLC with Different Sized Gaussian Membership Functions

In the previous sections, we have dealt with FLC having uniform sized membership functions. In pursuit to design a better FLC, the option of having different sized MFs was explored. In the equally sized Gaussian fuzzy set, it was observed that 25,686 samples out of the totally considered 60,003 samples i.e. 42% samples fell under the set [input-1=mf3, input-2=mf3 and output=mf3]. If equal number of samples represent each set, only 480 samples are expected in any set. This means that the number of samples in the considered set is 53 times the average number of samples in each set.

To avoid the above mentioned inequality in the sample distribution, there were two options:

- (a) Consider a different PID database to cater for equal distribution of samples in each of the 125 sets.
- (b) Change the size or parameters of each membership function such that the considered PID database automatically divides equal number of samples under each membership function(separate distribution for input-1, input-2 and output).

Choosing option(a) is almost impossible and so, option (b) was implemented. Here the size and parameters of each membership function of input-1, input-2 and output was customized as deemed necessary.

7.4.1 Procedure for Defining Parameters of Each Gaussian MF

- The entire PID database was arranged in the ascending order of input-1 values.
- Since there are 60,003 samples in total, the input-1 value of PID samples representing the Serial number 1, 12001, 24001, 36003, 48003 and 60003 were considered for calculating the limit points of each membership function.
- The same procedure was repeated for input-2 and output after respective ordering separately.
- The limit points of the 5 ranges is specified in the below table:

Table 7.6. Six limit points defining five ranges of various fuzzy sets

Sl No	Sl. No in the arranged PID database	Input-1	Input-2	Output
1	1	-4.3601	-13.6152	-30.0000
2	12001	-0.3628	-0.6534	-12.1135
3	24001	-0.0114	-0.0949	-2.5761
4	36003	0.0226	0.0886	2.4419
5	48003	0.3557	0.6340	12.1800
6	60003	4.0951	13.6779	30.0000

The six limit points give end points of five mfs of input-1, input-2 and output fuzzy sets. The center point of each Gaussian MF is the midpoint of its respective end points.

- The full width at 25% of maximum peak for a Gaussian is:

$$(2\sqrt{2\ln 4})c = 3.330218445c$$

where c is the standard deviation of the Gaussian curve.

- To ensure that the Gaussian curves overlap its adjacent MF at the 25% peak value height, we use the below formula:

$$\text{Full width at 25\% of maximum peak} = (3.330218445) c \quad (19)$$

Using the above formula, standard deviation and center point of each Gaussian MF is calculated and tabulated below:

Table 7.7. Parameters of different sized Gaussian MFs

Center point (b)				Standard Deviation (c)			
	Input-1	Input-2	Output		Input-1	Input-2	Output
mf1	-2.3615	-7.1343	-21.0568	mf1	1.20029	3.89215	5.37096
mf2	-0.1871	-0.3742	-7.3448	mf2	0.10552	0.16771	2.86391
mf3	0.0056	-0.0032	-0.0671	mf3	0.01020	0.05510	1.50681
mf4	0.1891	0.3613	7.3110	mf4	0.10004	0.16380	2.92415
mf5	2.2254	7.1560	21.0900	mf5	1.12286	3.91681	5.35100

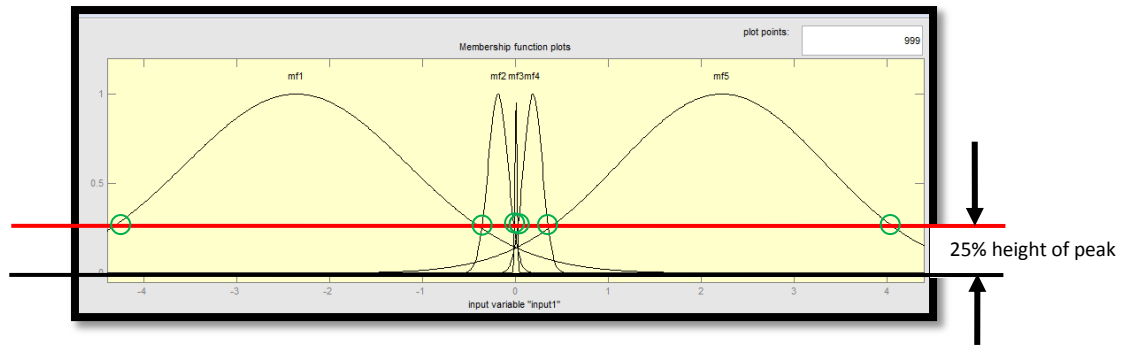


Fig 7.9 Fuzzy set with different sized Gaussian MFs intersecting at 25% peak height

In the above diagram, the red line indicates 0.25 height which is 25% height of '1' (maximum peak). It is very evident that all the Gaussian MFs intersect each other on the red line which is marked by green rings. The 5 ranges selected (one for each MF) is demarcated by the six green lines as shown in the figure below for input-1. All the 5 ranges marked by blue lines contain equal number of samples from PID database.

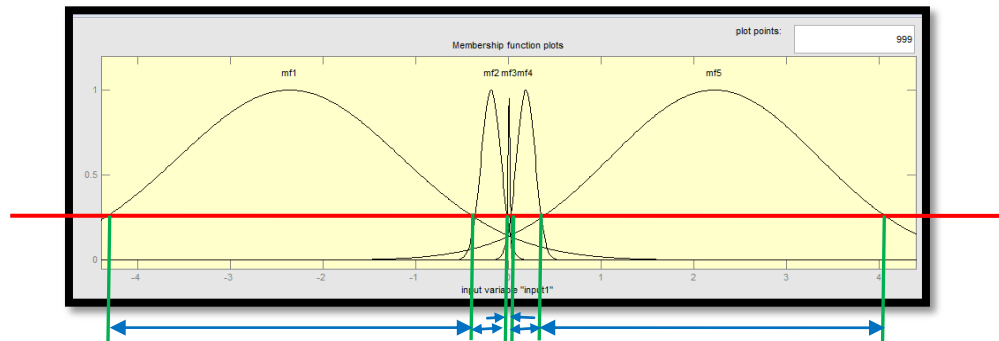


Fig 7.10 Figure showing MFs of various sizes but representing equal no. of PID samples

Number of PID samples falling between any two adjacent green lines is same. Similarly, MFs were calculated for input-2 and output to get the below figures:

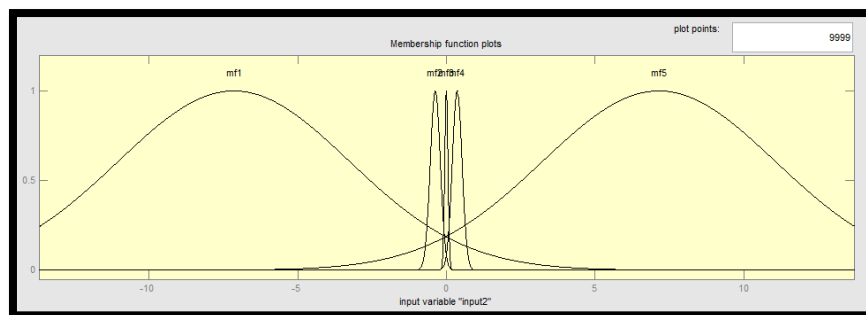


Fig 7.11 Fuzzy set of Input-2 with different sized MFs

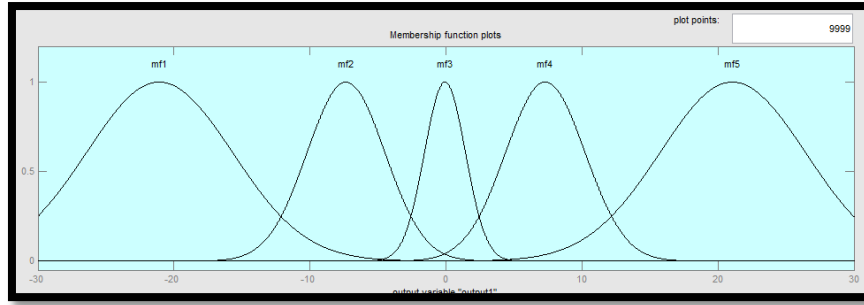


Fig 7.12 Fuzzy set of Output with different sized MFs

7.4.2 Methodology Used for Deriving Rules

- Input-1 of each sample in the PID database was assigned a MF based on the range in to which it falls..
- Same procedure was used to assign a MF for Input-2 and output of every sample in the PID database.
- Since there are 3 variables(input-1, input-2 and output) and each variable has 5 MFs, there are a total of $(5 \times 5 \times 5 =)$ 125 possible sets of combinations into which each sample will be segregated into based on its MF assignment.

Frequency of each set was calculated and tabulated at table 7.8.

Table 7.8. Grouping of PID database for rules creation of FLC with different sized MFs

Sl No	Membership Function of			Freq	Weigh-tage
	Ip-1	Ip-2	Op		
1	mf1	mf1	mf1	2308	0.6684
2	mf1	mf1	mf2	413	0.11961
3	mf1	mf1	mf3	260	0.0753
4	mf1	mf1	mf4	228	0.06603
5	mf1	mf1	mf5	259	0.07501
6	mf1	mf2	mf1	468	0.13553
7	mf1	mf2	mf2	938	0.27165
8	mf1	mf2	mf3	1096	0.31741
9	mf1	mf2	mf4	83	0.02404
10	mf1	mf2	mf5	8	0.00232
11	mf1	mf3	mf1	173	0.0501
12	mf1	mf3	mf2	753	0.21807
13	mf1	mf3	mf3	123	0.03562
14	mf1	mf3	mf4	8	0.00232
15	mf1	mf3	mf5	0	0

Sl No	Membership Function of			Freq	Weigh-tage
	Ip-1	Ip-2	Op		
16	mf1	mf4	mf1	621	0.17984
17	mf1	mf4	mf2	569	0.16478
18	mf1	mf4	mf3	52	0.01506
19	mf1	mf4	mf4	7	0.00203
20	mf1	mf4	mf5	0	0
21	mf1	mf5	mf1	3453	1
22	mf1	mf5	mf2	176	0.05097
23	mf1	mf5	mf3	5	0.00145
24	mf1	mf5	mf4	0	0
25	mf1	mf5	mf5	0	0
26	mf2	mf1	mf1	166	0.04807
27	mf2	mf1	mf2	833	0.24124
28	mf2	mf1	mf3	592	0.17145
29	mf2	mf1	mf4	497	0.14393
30	mf2	mf1	mf5	357	0.10339

Sl No	Membership Function of			Freq	Weigh-tage
	Ip-1	Ip-2	Op		
31	mf2	mf2	mf1	427	0.12366
32	mf2	mf2	mf2	709	0.20533
33	mf2	mf2	mf3	1075	0.31132
34	mf2	mf2	mf4	609	0.17637
35	mf2	mf2	mf5	237	0.06864
36	mf2	mf3	mf1	205	0.05937
37	mf2	mf3	mf2	387	0.11208
38	mf2	mf3	mf3	816	0.23632
39	mf2	mf3	mf4	299	0.08659
40	mf2	mf3	mf5	209	0.06053
41	mf2	mf4	mf1	224	0.06487
42	mf2	mf4	mf2	1221	0.35361
43	mf2	mf4	mf3	403	0.11671
44	mf2	mf4	mf4	150	0.04344
45	mf2	mf4	mf5	209	0.06053
46	mf2	mf5	mf1	921	0.26672
47	mf2	mf5	mf2	1271	0.36809
48	mf2	mf5	mf3	171	0.04952
49	mf2	mf5	mf4	10	0.0029
50	mf2	mf5	mf5	2	0.00058
51	mf3	mf1	mf1	5	0.00145
52	mf3	mf1	mf2	8	0.00232
53	mf3	mf1	mf3	77	0.0223
54	mf3	mf1	mf4	89	0.02577
55	mf3	mf1	mf5	81	0.02346
56	mf3	mf2	mf1	683	0.1978
57	mf3	mf2	mf2	467	0.13524
58	mf3	mf2	mf3	494	0.14306
59	mf3	mf2	mf4	561	0.16247
60	mf3	mf2	mf5	343	0.09933
61	mf3	mf3	mf1	758	0.21952
62	mf3	mf3	mf2	1445	0.41848
63	mf3	mf3	mf3	1531	0.44338
64	mf3	mf3	mf4	1658	0.48016
65	mf3	mf3	mf5	735	0.21286
66	mf3	mf4	mf1	350	0.10136
67	mf3	mf4	mf2	663	0.19201
68	mf3	mf4	mf3	535	0.15494
69	mf3	mf4	mf4	544	0.15754
70	mf3	mf4	mf5	739	0.21402
71	mf3	mf5	mf1	48	0.0139

Sl No	Membership Function of			Freq	Weigh-tage
	Ip-1	Ip-2	Op		
72	mf3	mf5	mf2	80	0.02317
73	mf3	mf5	mf3	83	0.02404
74	mf3	mf5	mf4	18	0.00521
75	mf3	mf5	mf5	7	0.00203
76	mf4	mf1	mf1	7	0.00203
77	mf4	mf1	mf2	31	0.00898
78	mf4	mf1	mf3	139	0.04025
79	mf4	mf1	mf4	1163	0.33681
80	mf4	mf1	mf5	912	0.26412
81	mf4	mf2	mf1	164	0.04749
82	mf4	mf2	mf2	102	0.02954
83	mf4	mf2	mf3	455	0.13177
84	mf4	mf2	mf4	1238	0.35853
85	mf4	mf2	mf5	203	0.05879
86	mf4	mf3	mf1	139	0.04025
87	mf4	mf3	mf2	235	0.06806
88	mf4	mf3	mf3	999	0.28931
89	mf4	mf3	mf4	353	0.10223
90	mf4	mf3	mf5	150	0.04344
91	mf4	mf4	mf1	298	0.0863
92	mf4	mf4	mf2	909	0.26325
93	mf4	mf4	mf3	1290	0.37359
94	mf4	mf4	mf4	599	0.17347
95	mf4	mf4	mf5	315	0.09123
96	mf4	mf5	mf1	339	0.09818
97	mf4	mf5	mf2	409	0.11845
98	mf4	mf5	mf3	484	0.14017
99	mf4	mf5	mf4	898	0.26006
100	mf4	mf5	mf5	168	0.04865
101	mf5	mf1	mf1	0	0
102	mf5	mf1	mf2	0	0
103	mf5	mf1	mf3	7	0.00203
104	mf5	mf1	mf4	220	0.06371
105	mf5	mf1	mf5	3349	0.96988
106	mf5	mf2	mf1	0	0
107	mf5	mf2	mf2	4	0.00116
108	mf5	mf2	mf3	38	0.011
109	mf5	mf2	mf4	858	0.24848
110	mf5	mf2	mf5	739	0.21402
111	mf5	mf3	mf1	0	0
112	mf5	mf3	mf2	11	0.00319

Sl No	Membership Function of			Freq	Weigh-tage
	Ip-1	Ip-2	Op		
113	mf5	mf3	mf3	165	0.04778
114	mf5	mf3	mf4	659	0.19085
115	mf5	mf3	mf5	192	0.0556
116	mf5	mf4	mf1	1	0.00029
117	mf5	mf4	mf2	71	0.02056
118	mf5	mf4	mf3	905	0.26209
119	mf5	mf4	mf4	856	0.2479

Sl No	Membership Function of			Freq	Weigh-tage
	Ip-1	Ip-2	Op		
120	mf5	mf4	mf5	468	0.13553
121	mf5	mf5	mf1	243	0.07037
122	mf5	mf5	mf2	295	0.08543
123	mf5	mf5	mf3	206	0.05966
124	mf5	mf5	mf4	396	0.11468
125	mf5	mf5	mf5	2318	0.6713

In table 7.8, we can clearly see that the maximum number of samples in any set is 3453 and is much lesser than that of table 7.3 (25,686). In the above table, frequency represents the number of samples of the PID database which fall under the set of the particular MF combination. Weightage is a number proportional to the frequency specified. This is the weightage applied to the rule. So, for example Sl. No 118 specifies a rule as:

"If (Error is mf5) AND (Roll rate is mf4), then (Control Signal is mf3)".

The weightage of this rule 0.26209. Accordingly, each of the 125 combinational sets specified in the table indicate a rule and we have 125 rules in total. However, out of these 125 rules, only 62 rules have non-zero weightage. These rules combine to give the following control surface:

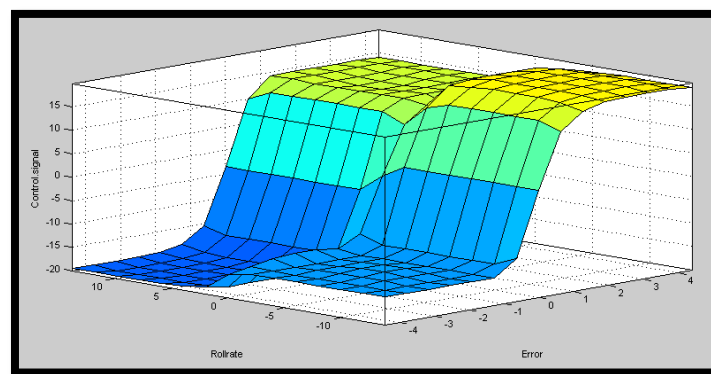


Fig 7.13 Control surface for FLC with different sized Gaussian MFs and 125 rules

7.4.3 FLC with 2-Inputs and 25 Rules. From the above table, separate FLC was designed with 25 rules. Here each combination of error and roll rate will be given a MF pertaining to the control signal with maximum samples(freq) from the PID database. The rule table is calculated as appended below:

Table 7.9. Fuzzy rules(25) of FLC with different sized Gaussian MFs

Control Signal		Roll rate				
		mf1	mf2	mf3	mf4	mf5
Error	mf1	mf1	mf3	mf2	mf1	mf1
	mf2	mf2	mf3	mf3	mf2	mf2
	mf3	mf4	mf1	mf4	mf5	mf3
	mf4	mf4	mf4	mf3	mf3	mf4
	mf5	mf5	mf4	mf4	mf3	mf5

The control surface is shown below:

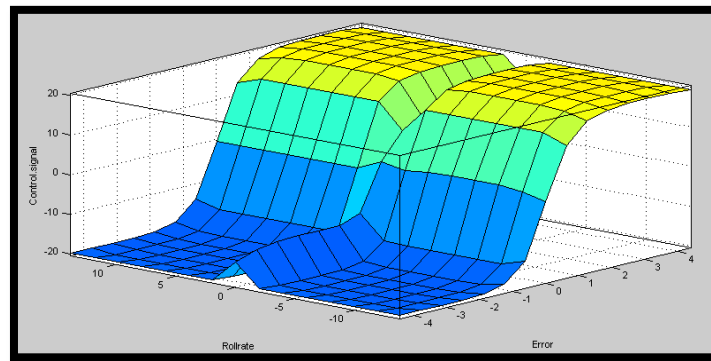


Fig 7.14 Control surface for FLC with different sized Gaussian MFs and 25 rules

The RMS value of ship's roll (A,B&C) was calculated separately using each of the above deigned FLC which has 5 / 25 / 125 rules and are tabulated below:

Table. 7.10. Ship's roll angle (RMS) using various FLCs with different sized Gaussian MFs

Ship's Roll (RMS)		No of rules in the FLC		
		5	25	125
Ship's Condition	A	10.823	5.1882	4.1317
	B	11.655	8.8774	6.1724
	C	13.4	7.0238	3.4419

7.5 FLC With Zero-Centered and Different Sized Gaussian MFs

In the previous section mf3 of input-1, input-2 and output fuzzy sets were not centered at '0'. So, the previously designed FLC with fuzzy sets containing different sized MFs and 125 rules was modified by adjusting the center points and standard deviations of all Gaussian MFs. Center points were adjusted so that center points of mf1 and mf2 are symmetric about vertical axis about '0' to that of mf4 and mf5 respectively. Center/peak point of mf3 is adjusted to be '0'. The rules designed for the last FLC designed were used for this FLC also. The RMS value of ship's roll (A,B&C) was calculated after using this FLC with 125 rules and is tabulated below:

Table. 7.11. RMS of Ship's roll using FLC with zero-centered and different sized MFs

<u>Ship's Condition</u>	<u>Ship's RMS roll angle (deg)</u>
A	5.1205
B	7.4844
C	4.2486

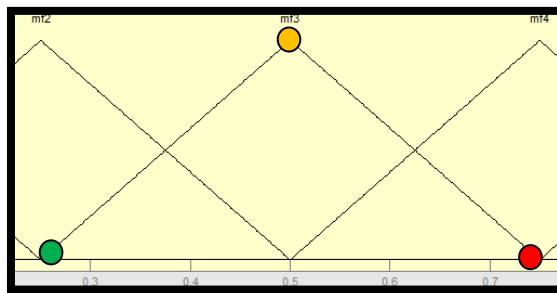
By analyzing table no.7.5, 7.10 and 7.11, it can be concluded that FLC designed with fuzzy sets containing same sized Gaussian MFs and 125 rules performed much better than other FLCs.

7.6 FLC with Different Sized Triangular MFs

Another FLC was designed using different sized triangular membership functions. As in the case of different sized Gaussian MFs designed earlier, the triangular MFs were also designed to ensure that each MF represents equal number of samples of the PID database. The left edge, right edge and the peak point's locations were precisely calculated to ensure that every triangle stretches and overlaps to its adjacent triangle by 25% of initial width of the adjacent triangle. The calculated values of centre point(peak), left edge and right edge of each triangular MF is tabulated below:

Table 7.12. Coordinates of the different sized triangular MFs

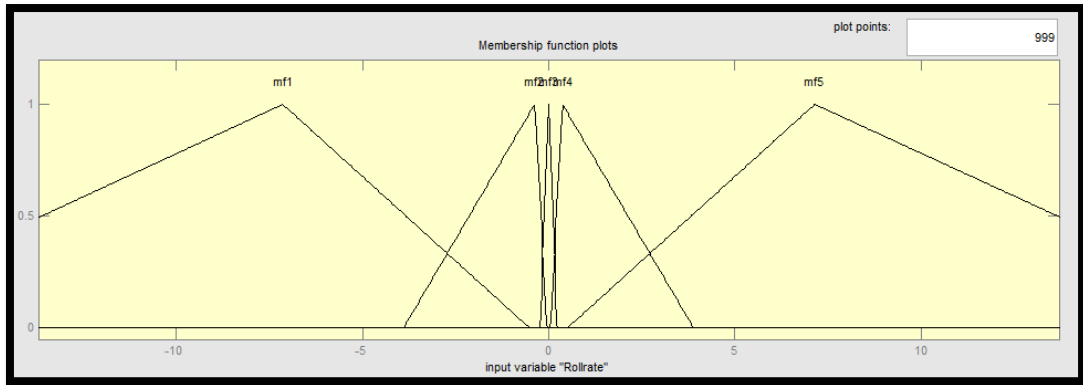
Center point/peak (●)			
	Ip-1	Ip-2	Op
mf1	-2.361	-7.134	-21.057
mf2	-0.187	-0.374	-7.345
mf3	0.006	-0.003	-0.067
mf4	0.189	0.361	7.311
mf5	2.225	7.156	21.090



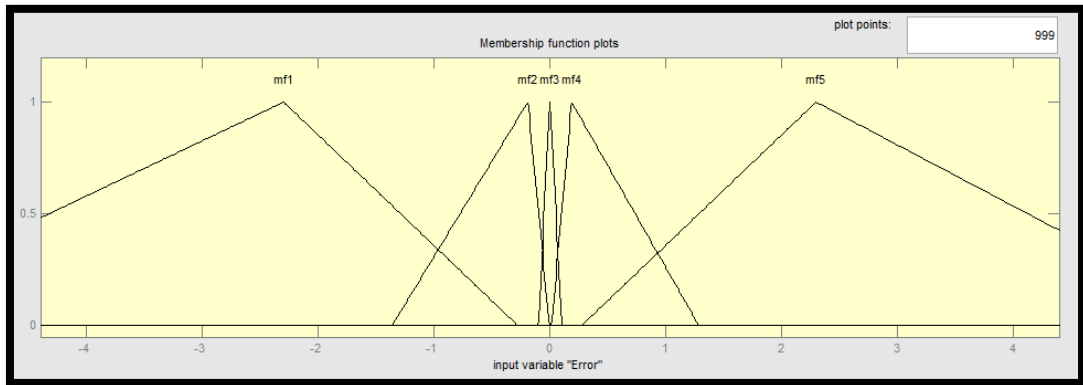
Left Edge(●)			
	Ip-1	Ip-2	Op
mf1	-6.359	-20.096	-38.943
mf2	-1.362	-3.894	-16.585
mf3	-0.099	-0.235	-4.960
mf4	0.014	0.043	1.187
mf5	0.272	0.498	9.745

Right Edge (●)			
	Ip-1	Ip-2	Op
mf1	-0.275	-0.514	-9.729
mf2	-0.003	-0.049	-1.322
mf3	0.106	0.225	4.876
mf4	1.291	3.895	16.635
mf5	5.965	20.200	38.910

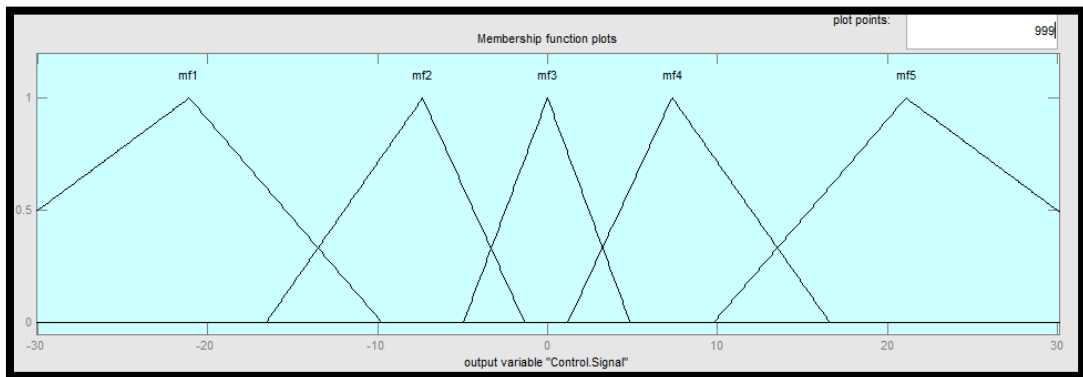
The fuzzy sets of the FLC are given at Fig.7.13:



(Input-1)



(Input-2)



(Output)

Fig 7.15 Fuzzy sets of Input-1,2 and Output of FLC with different sized triangular MFs

A total of 125 ruled were developed after detailed analysis of the PID database as it was done for Gaussian MFs. The control surface is shown at Fig.7.14:

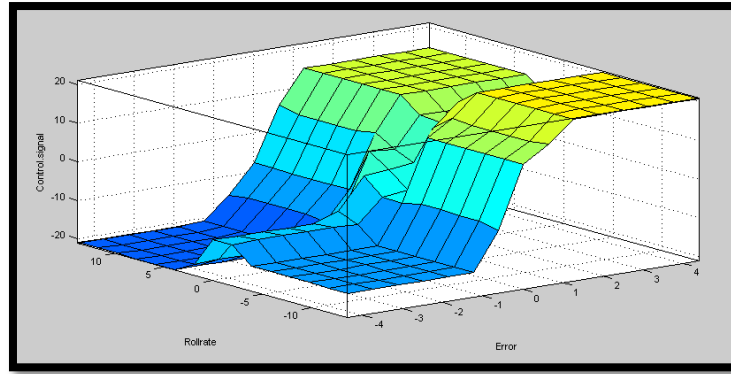


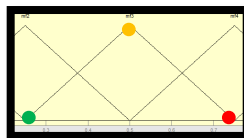
Fig 7.16 Control surface for FLC with different sized triangular MFs and 125 rules

7.7 FLC with Zero-Centered and Different Sized Triangular MFs

Another FLC was designed using fuzzy sets containing different sized triangular membership functions which are symmetric and zero-centered. The triangular MFs were also designed to ensure that each MF represents almost equal number of samples of the PID database. The left edge, right edge and the peak point's locations were precisely calculated to ensure that every triangle stretches and overlaps to its adjacent triangle by 25% of the original width of the adjacent triangle. The calculated values of centre point(peak), left edge and right edge of each triangular MF is tabulated below:

Table 7.13. Coordinates of the zero-centered and different sized triangular MFs

Center point/peak(●)			
	Ip-1	Ip-2	Op
mf1	-2.300	-7.140	-21.090
mf2	-0.189	-0.374	-7.345
mf3	0.000	0.000	0.000
mf4	0.189	0.374	7.345
mf5	2.300	7.140	21.090



Left Edge(●)			
	Ip-1	Ip-2	Op
mf1	-6.359	-20.096	-38.943
mf2	-1.362	-3.894	-16.585
mf3	-0.099	-0.235	-4.960
mf4	0.014	0.043	1.187
mf5	0.272	0.498	9.745

Right Edge(●)			
	Ip-1	Ip-2	Op
mf1	-0.275	-0.514	-9.729
mf2	-0.003	-0.049	-1.322
mf3	0.106	0.225	4.876
mf4	1.291	3.895	16.635
mf5	5.965	20.200	38.910

A total of 125 ruled were developed after detailed analysis of the PID database and it's rules are same as used for the FLC with different sized Triangular Membership Functions and shown in Fig 7.14. **FLC designed with non-centered and different sized triangular MFs performed better to the FLC designed with different sized and centered triangular MFs.** The RMS values of the ship's roll by using the above mentioned triangular functions is tabulated below along with two other FLCs designed earlier.

Table 7.14. Ship's roll angle (RMS) using various good performing FLCs

<u>Ship's Condition</u>	<u>Non-Centered Triangular MFs</u>	<u>Zero Centered Triangular MFs</u>	<u>Equally spaced Gaussian MFs</u>	<u>Different sized Gaussian MFs</u>
A	6.4281	6.4755	2.5971	4.1317
B	11.8489	11.8479	2.1237	6.1724
C	7.3917	8.3229	3.0687	3.4419

By analyzing the table 7.14, it is clear that the FLC designed with fuzzy sets containing equally spaced Gaussian membership functions and 125 rules performed better than all other FLCs designed.

Chapter 8

Particle Swarm Optimization (PSO)

8.1 Introduction

Particle swarm is a population-based algorithm. A collection of individuals called particles move in steps throughout a region. At each step, the algorithm evaluates the objective function at each particle. After this evaluation, the algorithm decides on the new velocity of each particle. The particles move, then the algorithm reevaluates.[34]

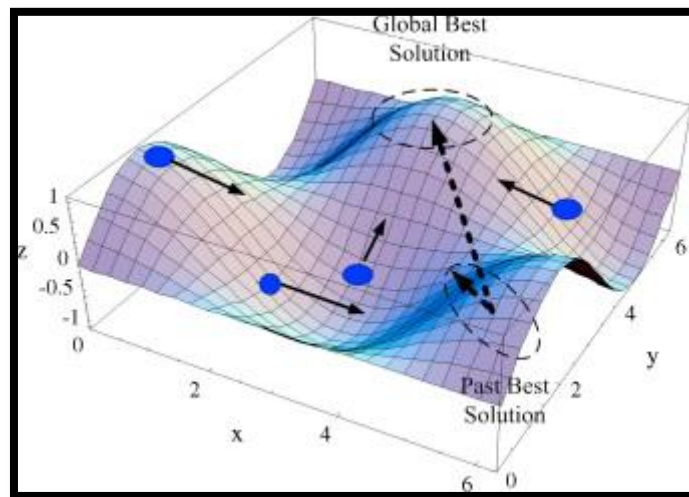


Fig 8.1 Graphical representation of particle shifting in PSO[35]

The inspiration for the algorithm is flocks of birds or insects swarming. Each particle is attracted to some degree to the best location it has found so far, and also to the best location any member of the swarm has found. After some steps, the population can coalesce around one location, or can coalesce around a few locations, or can continue to move. The particle swarm function attempts to optimize using a Particle Swarm Optimization Algorithm.[34]

8.2 PSO for tuning FLC gains. In the previous chapter, the FLC designed with equally spaced Gaussian membership functions and 125 rules was the best performing FLC in comparison to other FLCs designed. To fine tune the FLC, 3 gains were added in the system-for input-1 & input-2 entering FLC and for output of FLC.

The values of these gains were tuned using Particle swarm optimization to minimize the value of the ship's roll. 'Y' as defined below was considered as the optimization function which is to be minimized:

$$Y = (0.65 \times a) + (0.1 \times b) + (0.25 \times c)$$

Here, a, b & c are the RMS values of the ship's roll in condition 'A','B' and 'C' respectively. In the above formula, more weightage of 65% was given to condition 'A' as it is the normal mode of ship's sailing condition and the ship is expected to be in this condition for most of the time. Condition 'B' is the most stable condition and its variations in its roll is comparatively not dangerous and accordingly given a weightage of 10%. Condition 'C' is the most unstable and dangerous condition of the ship. However the ship is expected to sail in this condition rarely and was accordingly given a weightage of 25%.

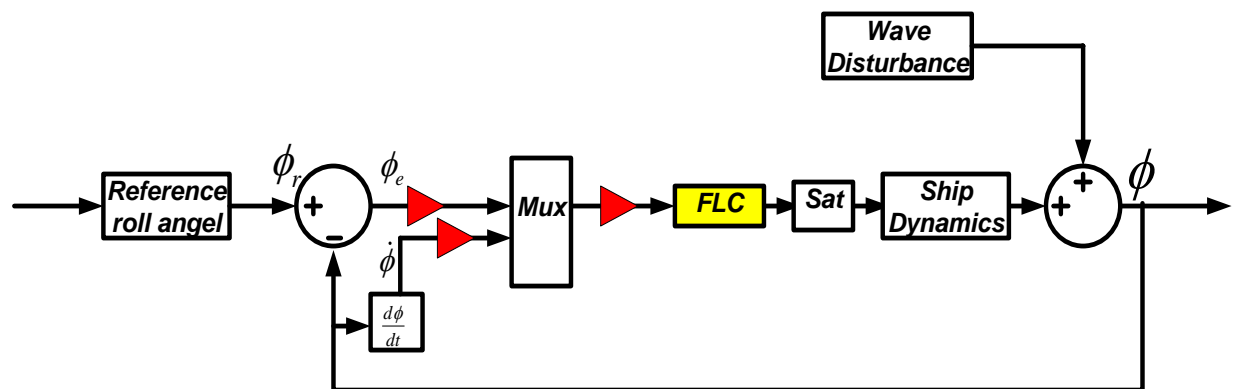


Fig 8.2 Block diagram of the system with saturated FLC and gains

PSO was used to minimize Y by optimizing the values of 3 gains mentioned earlier. Initially the range for the 3 variables was considered as '-100 to +100' and 100 particles were used during PSO. Subsequently, PSO was repeated by considering various ranges of the 3 variables/gains separately. The results of the PSO in terms of gain values and ship's roll are given in table. 8.1. The best / minimum value of Y was observed to be 2.2678 when lower & upper bound values for the gains were set at -3 & +3. The RMS values of ship's roll in conditions A,B and C was 2.229, 2.2809, 2.3792 respectively.

Table 8.1. Optimized Ship's roll angle with various particle ranges of PSO

Sl No	Lower Bound	Upper Bound	Optimized Gains for			Ship's roll in condition			Y
			Gain-1 (Input -1)	Gain-2 (Input -2)	Gain-3 (Output)	A	B	C	
1	-100	100	65.6226	-7.0336	58.8146	6.727	6.689	6.721	6.722
2	-50	50	-1.1760	-1.8930	-0.9348	2.198	2.298	2.527	2.290
3	-20	20	-1.0736	-1.7305	-0.9863	2.2324	2.337	2.411	2.287
4	-3	3	-1.1014	-1.5921	-1.0108	2.222	2.280	2.379	2.267
5	-2	2	-1.0709	-1.6803	-1.0692	2.163	2.703	2.440	2.286
6	-1	1	-0.9981	-1	-1	2.400	1.873	2.745	2.433

So as to observe the behavior and performance of PSO, Y was minimized by considering different number of particles ranging from 10 to 200 in PSO. Here the range of gain variables was fixed between -3 to 3. The results are tabulated in table 8.2.

Table 8.2. Optimised Ship's roll angle with different number of particle used in PSO

Sl No	LB	UB	No. of Particles	Optimised Gains for			Ship's roll (RMS) in condition			Y
				Gain-1 (Input-1)	Gain-1 (Input-2)	Gain-1 (Output)	A	B	C	
1	-3	3	10	-0.9016	1.6926	-1.006	2.622	2.510	3.122	2.7361
2	-3	3	20	1.0453	1.8924	0.9692	2.245	2.043	2.410	2.2663
3	-3	3	30	1.0786	1.9524	0.927	2.216	1.870	2.399	2.2275
4	-3	3	40	-1.0775	-1.7068	-0.9889	2.162	2.401	2.554	2.2845
5	-3	3	50	-1.1231	-1.5102	-0.9191	2.273	1.854	2.479	2.2832
6	-3	3	60	-1.0729	-1.7041	-0.9579	2.221	1.956	2.554	2.2783
7	-3	3	70	-1.0831	-1.5107	-0.9178	2.31	1.806	2.396	2.2871
8	-3	3	80	1.0578	1.8177	0.9794	2.175	2.093	2.380	2.2183
9	-3	3	90	1.1046	1.4998	0.9298	2.303	1.706	2.504	2.2943
10	-3	3	100	-1.1127	-1.5438	-0.9041	2.278	1.845	2.491	2.2886
11	-3	3	150	1.118	1.8412	0.9475	2.193	2.044	2.408	2.2319
12	-3	3	200	-1.1309	-1.4302	-0.9851	2.204	1.873	2.450	2.2326

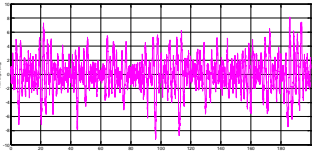
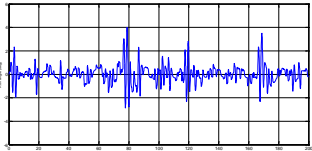
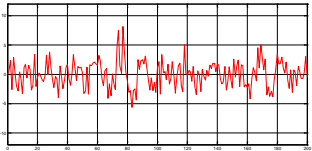
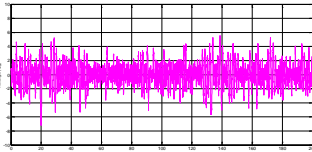
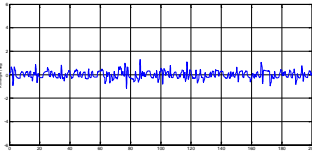
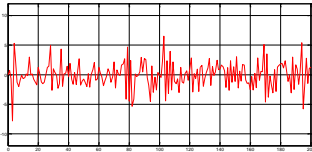
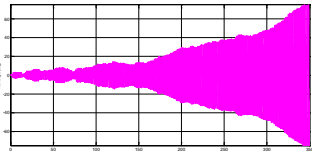
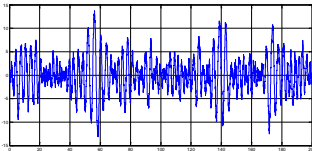
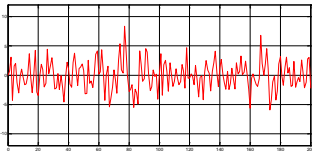
In the above process, the minimum value of Y was finally observed for gain values of 1.0578, 1.8177, and 0.9794. The minimizes value of 'Y' was 2.2183 and RMS angle of ship's roll in condition A, B & C was 2.1753, 2.093, 2.3803.

Chapter 9

Results And Analysis

Out of the many NN controlled designed in chapters 5 and 6, NN controller designed with 2 inputs, 28 hidden neurons and saturation limits considered in chapter 6 gave the best performance. Similarly, out of the many FLC designed using wide variety of MFs, the FLC designed with 2 inputs, 125 rules and equal sized & spaced Gaussian MFs gave the best performance. The FLC was later optimized by including gains which were tuned by particle swarm optimization(PSO). The ship's roll angle is plotted after using these finalised controllers and is tabulated below along with the finalised PID controller results:

Table 9.1. Roll angle comparison between finalised PID, NN and fuzzy logic controllers

		Ship's roll angles by using the finalised controllers		
		PID	Neural Network	FLC
Ship's Condition	A			
	B			
	B			

The ship's roll in terms of RMS and RSR values using the finalised PID controller, NN controller and fuzzy logic controller are tabulated below:

Table 9.2. Roll angle(RMS) comparison between finalised PID, NN and fuzzy logic controllers

<u>Ship's Condition</u>	<u>PID Controller (deg)</u>	<u>NN Controller (deg)</u>	<u>Fuzzy Logic controller (deg)</u>
A	2.4534	1.2264	2.1753
B	1.7111	0.3594	2.0930
C	8.8440	3.9782	2.3803

Table 9.3. Roll angle(RSR) comparison between finalised PID, NN and fuzzy logic controllers

<u>Ship's Condition</u>	<u>PID Controller (%)</u>	<u>NN Controller (%)</u>	<u>Fuzzy Logic controller (%)</u>
A	64.24	82.12	68.29
B	75.10	94.77	69.54
C	-28.64	42.14	65.38

By analyzing the above tables, one can draw the following results:

- Finalised NN controller and FLC performed better to PID controller in almost all the cases. However, performance of PID controller was better than FLC in ship's condition B.
- Comparing NN controller and FLC, NN performed better in ship's condition 'A' and 'B' whereas FLC performed better in ship's condition 'C'.
- Performance of FLC was less effected by the ship's condition in comparison to PID or NN controller.
- Even though, overall performance of NN controller seems better than the FLC, the roll cycles/min in case of FLC is much better than PID/NN controller. The same is tabulated in table 9.4.

Table 9.4. Roll frequency (per min) comparison between finalised PID, NN and FLC

<u>Ship's Condition</u>	<u>PID Controller (cycles/min)</u>	<u>NN Controller (cycles/min)</u>	<u>Fuzzy Logic controller (cycles/min)</u>
A	54	34.5	15
B	63	24	14.7
C	39	24.3	15.6

From table 9.4, it can be concluded that FLC provided lesser roll frequency. This is a big advantage which a controller can provide to a ship. Having more roll frequency is very detrimental to the performance of the crew and is also dangerous to the ship. Taking in to consideration that the ship is a Denmark fisheries ship, it is assumed that achieving less roll frequency is more important than decreasing roll angle by 1 or 2 degrees. So, controlling the ship's roll by using the designed FLC is much better than PID and NN controllers.

Chapter 10

Conclusion And Future Work

10.1 Conclusion

The marine vessels face a highly complex and dynamic situations at sea. Designing a classical controller like a PID controller with assumptions like ship having a fixed transfer function can be highly dangerous and can even sink ships. To control the roll motion of the considered ship, initially designed PID controller gave an acceptable performance under normal conditions. However, with changes in the ship's parameters, the roll motion deteriorated and even **sank the ship** in extreme conditions.

The stabilizer fins have saturation limits in respect to their fin angle and need to be considered while designing the control system. Not considering this is meaningless in practical terms. By considering the saturation limits, the effect of stabilizer fins reduce and roll angles will increase. However, this is what is practically feasible.

Among the various neural network controllers designed, NN control trained with 2 inputs, one target and 28 hidden neurons gave the best result. It's performance is better than the PID controller in almost all cases.

Among the many fuzzy logic controllers designed, the FLC designed with 2 inputs, 125 fuzzy rules with different weights and fuzzy sets with equally spaced & sized Gaussian membership functions performed the best. It's performance was improved by tuning the added gain values by particle swarm optimization(PSO) technique. Even though the overall performance of FLC in terms of the ship's roll angle is in-between the PID and NN controllers, the roll frequency (cycles/min) of FLC is much lesser and better than PID/NN controlled ships. So, one has to choose NN controller if achieving lesser roll angles is more important than achieving lesser roll frequency. Similarly, FLC is to be chosen if achieving lesser roll frequency is of more importance than the roll angle.

Even though the NN controller gave the least roll angles, its roll frequency is almost double the roll frequency of that of fuzzy logic controller. So, in the present considered ship, it is wise to choose FLC with much lesser roll frequency. Here accepting a 1 or 2 degree of extra roll angle than the NN controller is a safe bet for

the lesser roll frequency achieved. Had the ship considered in this dissertation been a heavily filled cargo vessel which prefers less roll angles over less roll frequency, NN controller can be chosen as it gave the least roll angles.

10.2 Future Scope

The future scope of the dissertation may include testing the methodologies used to create NN and FLC using the PID databases may be tried upon systems where training data and system control rules are known. Adaptive Neuro-Fuzzy Inference Systems (ANFIS) based controller may be designed for controlling the ship's roll and its performance may be evaluated in comparison to the controllers designed in this dissertation. Controller may be designed by considering more non-linearities to get better and practical controller.

Bibliography

- [1] T. Perez, *Ship motion control: course keeping and roll stabilisation using rudder and fins*: Springer Science & Business Media, 2006.
- [2] C.-Y. Tzeng and C.-Y. Wu, "On the design and analysis of ship stabilizing fin controller," *Journal of Marine Science and Technology*, vol. 8, pp. 117-124, 2000.
- [3] R. Bhattacharyya, *Dynamics of marine vehicles*: Wiley, 1978.
- [4] T. I. Fossen, *Guidance and control of ocean vehicles*: John Wiley & Sons Inc, 1994.
- [5] www.hoppe-marine.com.
- [6] T. Perez and M. Blanke, *Mathematical ship modelling for control applications*: Ørsted-DTU, Automation, 2002.
- [7] J. Van Amerongen and J. Van Cappelle, "Mathematical modelling for rudder roll stabilization," 1981.
- [8] G. Roberts, "Trends in marine control systems," *Annual reviews in control*, vol. 32, pp. 263-269, 2008.
- [9] "www.vdvelden.com."
- [10] R. Li, T. Li, W. Bai, and X. Du, "An adaptive neural network approach for ship roll stabilization via fin control," *Neurocomputing*, 2015.
- [11] S. Haykin and N. Network, "A comprehensive foundation," *Neural Networks*, vol. 2, 2004.
- [12] H. D. Fuat Alarçin, M Ertugrul Su, Ahmet Yurtseven, "Modified pid control design for roll fin actuator of nonlinear modelling of the fishing boat," *Polish Maritime Research*, vol. 21, pp. 3-8, 2014.
- [13] J. Chadwick, "On the stabilization of roll," 1900.
- [14] F. Alarçin, "Internal model control using neural network for ship roll stabilization," *Journal of marine science and technology*, vol. 15, pp. 141-147, 2007.
- [15] J. Hongzhang and X. Liang, "Ship Control Principle," ed: Harbin Engineering University Press, 2002.
- [16] S. Shuai, H. Jiangqiang, Y. Jianchuan, and J. Tao, "Design of simplified fuzzy controller for ship fin stabilizer," in *Control Conference (CCC), 2014 33rd Chinese*, 2014, pp. 4534-4538.
- [17] Z.-g. Qi, H.-z. Jin, W.-y. Liu, and Y. Xu, "Research on active fin stabilizer at low speed and its application to ship roll stabilization," in *OCEANS 2014-TAIPEI*, 2014, pp. 1-6.
- [18] K. Liu and Z. Zhang, "Design of fin stabilizer control system based on quantitative feedback theory," in *Computer Science & Education (ICCSE), 2014 9th International Conference on*, 2014, pp. 1032-1037.
- [19] S. Kuo-Ho, "Anti-rolling fin control for ship stabilization," in *Automatic Control Conference (CACS), 2013 CACS International*, 2013, pp. 389-394.
- [20] L. Kuang and Z. Zhiyang, "Design of fin stabilizer control system based on quantitative feedback theory," in *Computer Science & Education (ICCSE), 2014 9th International Conference on*, 2014, pp. 1032-1037.
- [21] J. Hongzhang, L. Zhiquan, Q. Zhigang, and J. Shuqiang, "Design of fin stabilizers control system with optimal added resistance," in *Control Conference (CCC), 2013 32nd Chinese*, 2013, pp. 7525-7529.
- [22] N. Hickey, M. Johnson, M. Katebi, and M. Grumble, "PID controller optimisation for fin roll stabilisation," in *Control Applications, 1999. Proceedings of the 1999 IEEE International Conference on*, 1999, pp. 1785-1790.
- [23] F. Alarçin, U. B. Celebi, S. Ekinçi, and D. Ünsalan, "Neural networks based analysis of ship roll stabilization," in *3rd International Conference on Maritime and Naval Science and Engineering*, 2010, pp. 217-220.
- [24] www.worldmaritimenews.com.

- [25] www.cruisedeals.expert.
- [26] www.soi.wide.ad.jp.
- [27] K. Ogata and Y. Yang, "Modern control engineering," 1970.
- [28] www.worldofdefense.blogspot.in.
- [29] www.dsalert.org.
- [30] www.bbauv.com.
- [31] www.nauticexpo.com.
- [32] P. Hájek, *Metamathematics of fuzzy logic* vol. 4: Springer Science & Business Media, 1998.
- [33] W. Pedrycz, *Fuzzy control and fuzzy systems (2nd: Research Studies Press Ltd., 1993*.
- [34] www.mathworks.com.
- [35] www.cssanalytics.wordpress.com.
- [36] I. Rivals and L. Personnaz, "Nonlinear internal model control using neural networks: application to processes with delay and design issues," *Neural Networks, IEEE Transactions on*, vol. 11, pp. 80-90, 2000.
- [37] L. Yan-Hua, J. Hong-Zhang, and L. Li-Hua, "Fuzzy PID Controller Lift Feedback Fin Stabilizer," *Marine Science Application*, pp. 127-134, 2008.
- [38] Z. Liu, H. Jin, M. J. Grimble, and R. Katebi, "Ship roll stabilization control with low speed loss," in *OCEANS 2014-TAIPEI*, 2014, pp. 1-6.
- [39] H. Li, S. Lu, C. Guo, and X. Li, "Adaptive fuzzy sliding mode controller design for ship fin stabilizer under rough sea conditions," in *Information and Automation (ICIA), 2014 IEEE International Conference on*, 2014, pp. 566-571.
- [40] L. Liang, B. Wang, S. Zhang, and P. Xun, "Stabilizer fin effect on SWATH ship motions and disturbance observer based control design," in *Mechatronics and Automation (ICMA), 2013 IEEE International Conference on*, 2013, pp. 1147-1152.
- [41] Z. Liu and H. Jin, "Modeling for ship roll-added-resistance and its application on fin stabilizer control system," in *OCEANS-Bergen, 2013 MTS/IEEE*, 2013, pp. 1-5.
- [42] S. Zhang, L. Liang, and J. Wang, "Analysis of real time stabilization effect and parameter optimization of fin stabilizer," in *Mechatronics and Automation (ICMA), 2012 International Conference on*, 2012, pp. 1103-1108.
- [43] H. Li, C. Guo, and D. Yin, "Hybrid control model of IMWNN and SNLC based on WNNI for ship fin stabilizer," in *Soft Computing and Pattern Recognition (SoCPaR), 2011 International Conference of*, 2011, pp. 312-317.
- [44] Y. Yang, X. Li, and L. H. Ke, "The Fuzzy Quantized Control of Fin Stabilizers under the Ship IPMS Networks," in *2010 Second International Conference on Intelligent Human-Machine Systems and Cybernetics*, 2010, pp. 3-6.
- [45] H. Li, C. Guo, and X. Li, "Ship roll stabilization using supervision control based on inverse model wavelet neural network," in *Intelligent Control and Automation (WCICA), 2010 8th World Congress on*, 2010, pp. 4829-4833.
- [46] S. Jiguang, J. Hongzhang, L. Lihua, and S. Hongyu, "Variable structure control based on grey prediction for ship fin stabilizer," in *Industrial Electronics, 2009. ISIE 2009. IEEE International Symposium on*, 2009, pp. 620-625.
- [47] R. Ghaemi, J. Sun, and I. V. Kolmanovsky, "Robust control of ship fin stabilizers subject to disturbances and constraints," in *American Control Conference, 2009. ACC'09.*, 2009, pp. 537-542.
- [48] H. Li, C. Guo, and H. Jin, "Hybrid control of inverse model wavelet neural network and PID and its application to fin stabilizer," in *Intelligent Control and Automation, 2006. WCICA 2006. The Sixth World Congress on*, 2006, pp. 436-440.
- [49] H. Li, C. Guo, and H. Jin, "Design of Adaptive Inverse Mode Wavelet Neural Network Controller of Fin Stabilizer," in *Neural Networks and Brain, 2005. ICNN&B'05. International Conference on*, 2005, pp. 1745-1748.

- [50] Z.-H. Xiu and G. Ren, "Fuzzy controller design and stability analysis for ship's lift-feedback-fin stabilizer," in *Intelligent Transportation Systems, 2003. Proceedings. 2003 IEEE*, 2003, pp. 1692-1697.
- [51] Y. Xuliang, Z. Haipeng, C. Fang, and J. Hongzhang, "Research on lift feedback fin stabilizer system and its intelligence controller," in *Control Applications, 2003. CCA 2003. Proceedings of 2003 IEEE Conference on*, 2003, pp. 966-971.
- [52] C. Shengzhong, L. Sheng, and S. Jingchuan, "Study of joint control system of main/flapped fin stabilizer," in *Electrical and Computer Engineering, 1999 IEEE Canadian Conference on*, 1999, pp. 896-901.
- [53] T. Perez and M. Blanke, "Ship roll damping control," *Annual Reviews in Control*, vol. 36, pp. 129-147, 2012.
- [54] A. J. Koshkouei and L. Nowak, "Stabilisation of ship roll motion via switched controllers," *Ocean Engineering*, vol. 49, pp. 66-75, 2012.
- [55] H. HAGHIGHI and M. R. JAHED-MOTLAGH, "Ship Roll Stabilization via Sliding Mode Control and Gyrostabilizer," *Bul. Inst. Polit. Iasi, LVIII*, 2012.
- [56] C. Kallstrom, P. Wessel, and S. Sjolander, "Roll reduction by rudder control," in *Ship Technology and Research Symposium (STAR), 13th*, 1900.
- [57] W. Froude, *On the rolling of ships*: Institution of Naval Architects, 1861.
- [58] S. Liu, J. Sun, and S. Chen, "Ship's fin stabilizer H/sup 8/ control under sea wave disturbance," in *Electrical and Computer Engineering, 1999 IEEE Canadian Conference on*, 1999, pp. 891-895 vol.2.
- [59] www.fmg.org.nz.
- [60] www.sciencemediacentre.co.nz.
- [61] www.turbosquid.com.
- [62] www.afma.gov.au.
- [63] www.clevernova.com.
- [64] www.ibiblio.org.
- [65] Available: https://www.google.co.in/?gfe_rd=cr&ei=-Hg7V97MLa-GgAXmplGoDg
- [66] www.nauticexpo.com.
- [67] H. Jin, Z. Liu, Z. Qi, and S. Jiang, "Design of fin stabilizers control system with optimal added resistance," in *Proceedings of the 32nd Chinese Control Conference*.
- [68] www.dieselship.com.
- [69] www.hoppe-marine.com.